Divergent ecological selection causes partial reproductive isolation and vast genomic instability in yeast

Running head: Ecological isolation barriers in yeast

*Devin P. Bendixsen[1,2], Ciaran Gilchrist[1], Chloé Haberkorn[1], Karl Persson[3], Cecilia Geijer[3], Jonas Warringer[4], Rike Stelkens[1]**

[1] Department of Zoology, Stockholm University, Svante Arrheniusväg 18 B, 106 91 Stockholm, Sweden

[2] MRC Human Genetics Unit, Institute of Genetics and Cancer, University of Edinburgh, Edinburgh, UK

[3] Division of Industrial Biotechnology, Department of Life Sciences, Chalmers University of Technology, Kemigården 1, 412 96 Göteborg, Sweden

[4] Department of Chemistry and Molecular Biology, University of Gothenburg, Medicinaregatan 9C, 41390 Göteborg, Sweden

* Corresponding author: Rike Stelkens, Department of Zoology Stockholm University, telephone: +46 (0) 816 4223; email: rike.stelkens@zoologi.su.se

Devin Bendixsen: 0000-0003-0831-7646; devin.bendixsen@gmail.com

Ciaran Gilchrist: 0000-0002-7639-6131; ciaran.gilchrist@umu.se

Chloé Haberkorn: 0000-0002-7371-9177; chloe.haberkorn@zoologi.su.se

Karl Persson: 0000-0002-2173-8165; karperss@chalmers.se

Cecilia Geijer: 0000-0002-4158-2938; cecilia.geijer@chalmers.se

Jonas Warringer: 0000-0001-6144-2740; jonas.warringer@cmb.gu.se

Rike Stelkens: 0000-0002-8530-0656; rike.stelkens@zoologi.su.se

Abstract

Populations evolving independently in divergent environments accumulate genetic differences and potentially evolve reproductive isolation as a by-product of divergence. The speed and mechanisms underlying this process are difficult to investigate because we rarely get the opportunity to witness them in natural settings, and histories of selection and gene flow between populations are often unknown. Here, we experimentally evolved yeast for 1000 generations of evolution in both divergent and parallel environments. At regular time points during experimental evolution, we made crosses between parallel- and divergent-evolving populations to measure postzygotic reproductive isolation (gamete viability). We used whole genome population sequencing to determine the mutational load, the number and types of structural variation, and other genomic features of the parent, F1, and F2 intraspecific hybrids. We found evidence for large scale phenotypic and genome-wide differentiation in response to divergent laboratory selection. Divergent-selected populations produced hybrids with reduced gamete viability - a classic signature of postzygotic reproductive isolation in the form of hybrid breakdown. Parallel-selected populations on the other hand remained reproductively compatible. We found that F2 hybrid genomes contained vast genomic instability, i.e., new structural variants (especially insertions, deletions, and interchromosomal translocations) that were not observed in parent and F1 genomes, which is likely a result of chromosome missegregation and recombination errors in hybrid meiosis. Our results provide phenotypic and genomic evidence that partial reproductive isolation evolved due to adaptation to divergent environments, consistent with predictions of ecological speciation theory.

Keywords: experimental evolution, hybridization, mutational load, reproductive isolation, *Saccharomyces,* structural variation

Introduction

Ecological speciation implies a process by which adaptation to different ecological niches, in allopatry or sympatry, leads to the evolution of reproductive isolation between populations (Mayr 1947; Schluter 2001; McKinnon et al. 2004; Nosil 2012). Long-term monitoring of natural populations has been valuable in linking ecological traits with the emergence of reproductive barriers (e.g. (Filchak et al. 2000; Rundle et al. 2000; Grant and Grant 2003; Funk et al. 2006; Sawada et al. 2022)), providing convincing arguments for ecological factors to play a role in driving population divergence. However, ecological speciation remains difficult to demonstrate because it usually proceeds over extended evolutionary times (Hendry et al. 2007), trait divergence is often cryptic (Struck et al. 2018; Sparks et al. 2022), and the evolutionary histories of natural populations are challenging to reconstruct. It is usually unknown whether divergent selection was present, how long it lasted, and what the timing and amount of gene flow was between populations. Thus, it often remains unclear, especially between allopatric species pairs occupying different niches, whether selection was the driving force underlying their divergence, eventually leading to speciation (Anderson and Weir 2022; Irestedt et al.; Müller et al.). Due to these constraints, studies have often relied on combinatorial approaches, using i) data on niche divergence in traits related to habitat use, such as resource utilization or foraging behavior (e.g. (Hatfield and Schluter 1999; Nosil and Crespi 2006; Munar-Delgado et al. 2024), ii) data on reproductive barriers, such as differences in mating behaviors or flowering times reducing gene flow between populations adapted to different ecological niches (e.g. (Dieckmann et al. 2004; Villa et al. 2019)), and iii) genetic data, detecting signatures of selection and divergence in genetic regions associated with ecological adaptation and reproductive isolation (e.g. (Nosil and Schluter 2011; Härer et al. 2021; Louder et al. 2024)).

Microbial experimental evolution provides a powerful tool for investigating questions in evolutionary biology. It has been used to describe the dynamics and genetic mechanisms underlying adaptation to stable (Lenski et al. 1991; Good et al. 2017; Johnson and Desai 2022), heterogenous

72 (Rainey and Travisano 1998), or changing environments (Bell and Gonzalez 2011; Gorter et al. 2016;
73 Gorter et al. 2017) and to test theoretical predictions about adaptation rates in sexual versus asexual
74 populations (McDonald et al. 2016; Kosheleva and Desai 2018; Leu et al. 2020). Experimental evolution
75 with microbes can also provide insights on fundamental questions in speciation, especially about the
76 early stages of divergence, i.e. why, how and when lineages split (Stelkens 2024). Microbial genomes are
77 often small and generation times are short, allowing for evolve-and-resequencing approaches to capture
78 speciation and its underlying genetic basis in action. For instance, experimental evolution with a virus
79 (lambda bacteriophage) and its bacterial host (*Escherichia coli*) has demonstrated that divergent
80 ecological selection caused the phages to split into two genetically distinct lineages with different host
81 preferences, and that barriers to gene flow formed as a consequence of ecological specialization, which
82 resulted in reproductive isolation (Meyer et al. 2016). Experiments with yeast and other fungi have
83 shown that divergent selection can lead to phenotypic divergence and rapid ecological differentiation
84 (Dettman et al. 2007; Dettman et al. 2008; Ament-Velásquez et al. 2022), even under high rates of gene
85 flow (Tusso et al. 2021). But generally, there is a lack of studies that combine both organismal and
86 genetic approaches to measure reproductive isolation (Westram et al. 2022). Especially work
87 investigating the emergence and dynamics of reproductive isolation using repeated measures of hybrid
88 viability across generational time scales, from the beginning to later stages of parental divergence under
89 controlled environmental conditions, could significantly advance our understanding of what drives the
90 evolution of reproductive isolation in the early stages of speciation.

91 Here, we used experimental evolution with the budding yeast *Saccharomyces cerevisiae* and
92 propagated replicate, asexually reproducing populations in both different and parallel (same)
93 environments for 1000 mitotic generations (**Figure 1**). At regular time points of population divergence,
94 we generated sexual F1 and F2 (hybrid) crosses between and within environments, to test whether
95 reproductive isolation evolved and increased with time. We profiled parental phenotypes in 90 different

96 environments to test for phenotypic divergence over time, and used whole genome sequencing on
97 parental, F1, and F2 hybrid populations to measure their mutational load and other measures of
98 genomic stability. By the endpoint of experimental evolution, we found that divergent-selected
99 populations were up to 50% reproductively isolated due reduced hybrid gamete viability, while crosses
100 made between parallel-selected populations remained genetically compatible. We detected vast
101 structural variation in the F2 hybrid genomes, including up to three times more deletions, insertions,
102 inversions, tandem duplications, and interchromosomal translocations than in the diploid parental and
103 F1 hybrid genomes. Together, our results suggest that structural genetic differences accumulating in
104 populations under divergent ecological selection led to severe genomic instability in hybrid genomes
105 due to recombination errors and chromosome missegregation which caused reproductive isolation,
106 consistent with predictions of ecological speciation theory.
107

108 **Materials and Methods**

109 ***Founder populations***

110 We generated large diploid, and genetically diverse, founder populations of yeast through mating and
111 mass sporulation of two *S. cerevisiae* strains (SK1 and Y55; Figure 1) as previously described (Ament-
112 Velásquez et al. 2022). SK1 and Y55 are relatively closely related and high quality reference genomes
113 are available for both (Peter et al. 2018; Devin P Bendixsen et al. 2021). Briefly, SK1 and Y55 were
114 genetically modified to introduce auxotrophies, which could be used as selective markers to exclude
115 non-mated haploids (non-hybrids). The founders of populations (called "N founder" below) evolving in
116 sodium chloride (NaCl) are the diploid recombined offspring of a cross between SK1 (MATα ho:KanMX
117 ura3::ClonNat) and Y55 (MATa ho leu2::HygMX ura3::ClonNat). All other founders (called "LE founder"
118 below) of the populations evolving in ethanol and two different concentrations of lithium acetate, are

119 the diploid recombined offspring of a cross between SK1 (MATα ho:KanMX lys2::ClonNat) and Y55
120 (MATa ho leu2::HygMX lys2::ClonNat).
121
122 ***Experimental evolution of parental populations***
123 From these founders, replicate populations (from here on 'parental´ populations) were experimentally
124 evolved in four different (divergent) and same (parallel) environments, in four independent replicates
125 each, for up to 1000 asexual generations (**Figure 1**). The number of generations was estimated by
126 counting cells after 48h growth in selective media in the highest stress environment (0.75M NaCl, see
127 Ament-Velásquez et al. 2022). This approach is conservative because it likely underestimates the
128 number of generations in the other, less stressful environments. All evolution environments contained
129 synthetic complete (SC) medium (2% glucose, 0.67% bacto-yeast nitrogen base without amino acids,
130 0.00079% Formedium CSM powder (product code DCS0019), made up to 1L with sterilised deionised
131 water) plus one of the following substances to induce stress: 0.75M sodium chloride (from here on
132 NaCl), 8% ethanol (C_2H_6O, from here on EtOH), and two different concentrations of lithium acetate
133 ($C_2H_3LiO_2$, from here on LiAc0.01M and LiAc0.02M). The correct volume of EtOH was added to the test
134 tube just before inoculation to limit evaporation. We have previously demonstrated that these four
135 media significantly differ in how much they reduce the fitness of populations, and we have provided
136 phenotypic and genetic evidence that populations become differentially adapted to these environments
137 (Ament-Velásquez et al. 2022).
138 Three to four replicate populations were evolved in separate test tubes containing 5mL of SC
139 media with one of the four substances. Then, we serially transferred 10µL of yeast culture every 48
140 hours to fresh media (approximately seven generations, estimated by counting cells after 48 hours).
141 Every five transfers (10 days, i.e. ~35 generations), a 900µL sample of each population was frozen in 44%
142 glycerol at -70°C for later use. The experiment was run for a total of ~300 days. After some cross-

replicate contamination was detected using sequencing data (Ament-Velásquez et al. 2022), we excluded two NaCl-evolved replicate populations (R1 and R4) at 1000 generations, all LiAc0.01M and LiAc0.02M-evolved populations at 1000 generations, and one LiAc0.01M-evolved population (R3) at all generations. No crosses were generated from these populations. Retained populations showed no signs of cross-contamination in terms of shared single nucleotide variants.

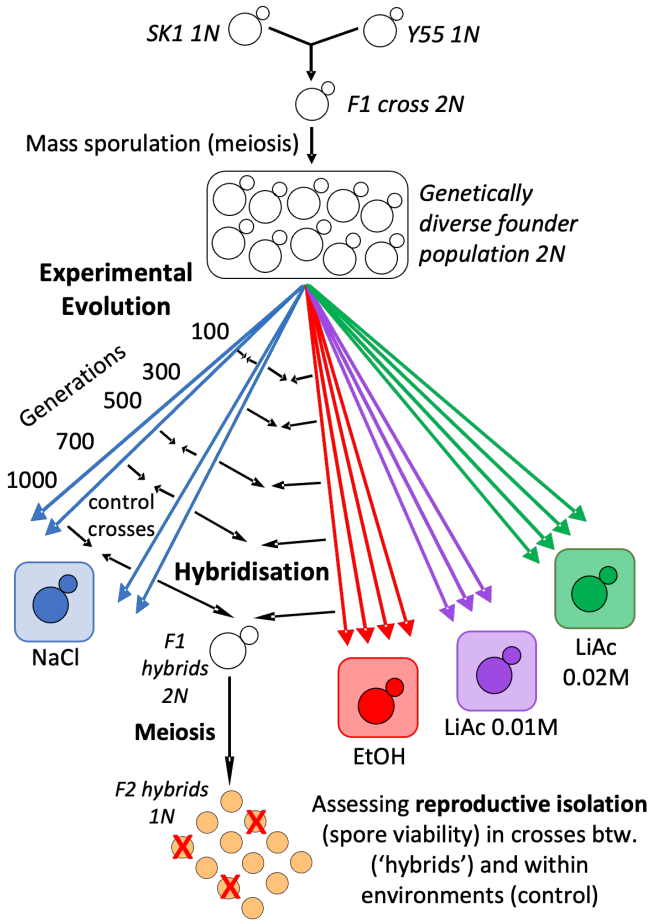

Figure 1: Experimental Design. A founder population was generated by the mating of two *S. cerevisiae* strains (SK1 and Y55), followed by mass sporulation (meiosis). This genetically diverse, diploid founder was split into four different environments, containing growth medium with either 0.75M NaCl, 8% EtOH, 0.01M lithium acetate, or 0.02M lithium acetate, and evolved for up to 1000 asexual generations by serial transfer, in three or four independent biological replicates per environment (Ament-Velásquez et al. 2022). At seven time points of divergence between these 'parent' populations, sexual hybrid crosses were made between NaCl-populations and populations from all other environments (with replication). Control crosses were made between populations evolving in parallel, in the same environment. All crosses were then sporulated and the viability of the haploid F2 offspring was assessed after tetrad dissection. 2N indicates diploid, 1N indicates haploid genotypes.

160 ***Hybridization at increasing timepoints of parental divergence***

161 We generated hybrid crosses at 100, 300, 500, 700, and 1000 generations of parental divergence,
162 between all four replicate NaCl-populations and up to four replicate populations from each of the three
163 other environments (LiAc 0.01M (3 replicates), LiAc 0.02M (4 replicates) and EtOH (4 replicates); **Figure**
164 **1**). Due to the selectable markers present in the parents, NaCl- populations could be mass-crossed with
165 the other three populations while safely removing all non-hybrid parental genotypes using a selective
166 medium (described below). First, we mass-sporulated the diploid parental populations. For this, 500µL
167 of saturated culture were added to 50mL of sporulation medium (1% potassium acetate, 0.05% glucose,
168 0.1% yeast extract, and H_2O to 1L) and left for 5 days with gentle shaking at room temperature. We then
169 mixed 500µL of each of the two parent spore cultures together in a 1.5mL Eppendorf tube, and
170 centrifuged the culture down to a pellet to induce mating. To select for F1 hybrids, we inoculated 25µL
171 of the pellet in 5mL of -lys SD medium with G418 (0.67% bacto-yeast nitrogen base without amino acids,
172 2% glucose, dropout powder (-lys), G418 400mgL^{-1} and H_2O to 1L). This selects for F1 hybrid genotypes
173 in bulk, which are heterozygous for both selective markers (-lys and G418). Note that this mass mating
174 and sporulation protocol permitted F1 hybrid populations to contain genetic diversity, depending on
175 how many different parental genotypes participated in the mass mating. To generate F2 hybrid
176 populations, we put F1 hybrid populations through one round of meiosis by mass sporulating them in
177 50mL of sporulation medium for 5 days with gentle shaking at room temperature. F1 AND F2 hybrid
178 populations were stored at -70°C in 22% glycerol solution for whole genome sequencing.

179

180 ***Assessing parental phenotypic divergence***

181 We phenotypically profiled all parent populations (i.e. populations evolved in NaCl, LiAc 0.01M, LiAc
182 0.02M, and EtOH) in 90 different environments, at increasing times of divergence, using the Scan-o-
183 Matic system for high-throughput microbial phenotyping (Zackrisson et al. 2016; Li et al. 2019; Alalam et

184 al. 2020; Mukherjee et al. 2021; Persson et al. 2022; Stenberg et al. 2022) version 2.2
185 (https://github.com/Scan-o-Matic/scanomatic.git). Parental populations were precultured in SC media
186 for 48h in 96-well plates at 30°C without shaking and frozen. Then, cultures were pinned directly from
187 thawed cryo-stocks in 96-format for preculturing on agar plates (for more detailed methods see
188 (Persson et al. 2024)). Samples were split into duplicates (two 96-well plates). A third plate was used for
189 propagation of a spatial control, containing a Y55 diploid strain. After preculture, populations were
190 pinned onto 1536 colony arrays on agar plates robotically (Singer ROTOR HDA), allowing for accurate
191 measuring of colony growth using the Scan-o-matic software. The spatial control was placed in every
192 fourth position (in total 384 colonies per plate) to remove any spatial bias, irregularities in the plates, or
193 other bias from the local area. In total, 52 distinct stressors were used in different concentrations,
194 resulting in 90 distinct environments, including superoxidative stress (e.g. paraquat), heavy metals (e.g.
195 $CuSO_4$), different carbon sources (e.g. maltose), antifungal drugs (e.g. Clotrimazole). Phenotypic data, i.e.
196 growth measurements, are reported in Table S1, with the full list of environments in Table S2.
197 Cultivation plates were maintained undisturbed and without lids for the entire duration of the assay
198 (72h) in high-resolution desktop scanners (Epson Perfection V800 PHOTO scanners, Epson Corporation,
199 UK) at 30°C, in moisture-controlled thermostatic cabinets with air circulation. We imaged plates at 20-
200 minute intervals using transmissive scanning at 600 dpi and extracted intensities for pixels included in,
201 and outside, each colony. We estimated the sum pixel intensity for each colony, subtracted the median
202 pixel intensity of the local background, and transformed the remaining cell-associated pixel intensity to
203 cell counts by using a pre-established calibration function, established using both spectrometry and flow
204 cytometry (Zackrisson et al. 2016). We smoothed and quality-controlled growth curves, rejecting
205 approximately 0.3% of growth curves as erroneous, blind with respect to sample identities. Based on the
206 number of cells after 72h, we used the yield normalized against the spatial control (Y55 diploid).

207 A custom 'ParentalDivergence' function was generated in R, using normalized yield, the number
208 of generations in experimental evolution, and the type of population comparison. Mean and double
209 standard deviations of normalized yields were first computed for each of the 90 environments for each
210 of the replicate parent 1 (P1) and 2 (P2) populations. This was done for each type of population
211 comparison, i.e. divergent-environment comparisons (NaCl x EtOH, NaCl x LiAc0.01, NaCl x LiAc0.02) and
212 parallel-environment comparisons (NaCl x NaCl, EtOH x EtOH, LiAc0.01 x LiAc0.01, LiAc0.02 x LiAc0.02).
213 We considered fitness to be higher if the normalized mean yield of P2 was larger than the normalized
214 mean yield of P1 plus P1's double standard deviation (i.e. mean P2 > mean P1 + 2σ). We considered
215 fitness to be lower if the normalized mean yield of P2 was lower than the normalized mean yield of P1
216 minus P1's double standard deviation, following previous protocols (i.e. mean P2 < mean P1 - 2σ; see
217 (deVicente and Tanksley 1993; Brice et al. 2021). Parental phenotypic divergence is thus defined as the
218 proportion of the 90 environments in which there was a large difference in yield between the two
219 populations compared.
220
221 ***Assessing reproductive isolation***
222 To assess the presence and degree of reproductive isolation between the parental yeast populations
223 evolving in divergent environments, we mated individual parent genotypes after 100, 300, 500, 700 and
224 1000 generations of experimental evolution. The crosses were plated onto solid YPD agar medium (1%
225 yeast extract, 2% peptone, 2% glucose, 2% agar made up to 1L with sterilized deionized H_2O) and grown
226 for 2 days, followed by replica plating onto solid KAc medium (1% potassium acetate, 0.05% glucose,
227 0.1% yeast extract and H_2O to 1L) for sporulation. Populations were left for 2-7 days, until tetrads were
228 identified under the microscope. Yeast tetrads usually contain four spores (gametes), which are the
229 recombined haploid products of meiosis. Sporulated cultures with tetrads were incubated for one hour
230 at room temperature in 10µL of filter sterilized zymolyase solution (1mg of zymolyase per 1mL of 1M

231 sorbitol solution) to kill vegetative (unsporulated) cells and digest the outer membrane of the tetrads,
232 surrounding the ascospores. Cell lysis was terminated by adding 500µL of sterilized H_2O. To assess the
233 fertility of F1 hybrid crosses at increasing timepoints of parental divergence, we dissected 10-20
234 individual F1 tetrads, and measured the survival rates of their haploid F2 offspring. Tetrads were
235 dissected on YPD plates using a Singer MSM 400 robot. Individual spores were then left to germinate
236 and grow for 72h at 30°C, at which point spore viability was assessed. Spores were counted as viable
237 based on the presence of colonies visible to the eye. Thus gamete viability was assessed as the capacity
238 to germinate and show sufficient growth to form macroscopic colonies. The total proportion of unviable
239 spores per cross was calculated from 20 dissected tetrads (80 spores) at 100, 700, and 1000 generations,
240 and 10 tetrads (40 spores) at 300 and 500 generations of parental divergence.
241 We also measured the F1 fertility of the control crosses, i.e. crosses between replicate parental
242 populations that evolved in parallel environments. We used the same mating, sporulation and dissection
243 protocols as described above. The total proportion of unviable spores (gametes) per cross was
244 calculated from 10 dissected tetrads (40 spores) at 100, 500, 700 and 1000 generations of parental
245 divergence.
246
247 ***DNA extraction and whole-genome sequencing***
248 DNA was extracted as described in (Ament-Velásquez et al. 2022). We extracted DNA from whole
249 parental, F1, and F2 hybrid populations, respectively, at seven time points each (0, 100, 200, 300, 400,
250 500, 700, and 1000 generations). Extraction was carried out on overnight culture, with ~1mL of culture
251 used. Library preparation and sequencing were performed at the Science for Life Laboratories
252 (Stockholm, Sweden), using the Illumina Nextera Flex protocol. Sequencing was done using either
253 NovaSeq S4-300 (2x150bp) or NovaSeq S-Prime (2x150bp) to an estimated median depth of coverage
254 per sample of around 30x to 780x. The raw sequences were deposited in the European Nucleotide

255 Archive, parental populations are available at accession number PRJEB46680, while hybrids are available
256 at accession number PRJEB83568.
257
258 ***Sequencing read quality and genome alignment***
259 FastQC v.0.11.9 (Andrews 2010) was used to assess the quality of raw sequencing reads and reads were
260 trimmed using Trimmomatic v0.36 (Bolger et al. 2014). Sequencing reads were aligned to a S288C
261 reference genome (R64; GenBank accession GCA_000146045.2) using BWA mem v0.7.17-r1188 (Li and
262 Durbin 2009) and SAMtools v1.11 (Danecek et al. 2021) was used to sort and index the resulting
263 mapping file. Duplicated reads were flagged and removed using Picard v3.1.0
264 (http://broadinstitute.github.io/picard/), followed by quality assessment using Qualimap v2.3
265 (Okonechnikov et al. 2016).
266
267 ***Assessing the genomic mutational landscape***
268 To assess the mutational landscape of each experimentally evolved, parental yeast population and the
269 F1 and F2 crosses made between them, we measured the amount of variants detected across
270 mutational scales, ranging from single nucleotide variants to entire chromosome aneuploidies. To
271 identify small mutational variants (SNV and indels), we used freebayes v1.3.6 (Garrison and Marth 2012)
272 with default parameters. Identified variants were filtered using VCFtools v0.1.16 (Danecek et al. 2011) to
273 include only variants with minimum quality (minQ) >30 and sequencing read depth (minDP) >5. SnpEff
274 v5.2 (Cingolani et al. 2012) was used to assess and annotate the effect of identified mutational variants
275 on genes using the database of the reference genome R64-1-1.105 with canonical transcripts. To
276 identify structural variants including insertions, deletions, inversions, tandem duplications and
277 interchromosomal translocations we used Manta v1.6.0 (Chen et al. 2016) with default parameters.
278 Structural variant detection is limited by the read pair fragment size. To more comprehensively assess

279 the genome-wide copy number variation (amplifications and deletions), we used Control-FREEC v11.6
280 (Boeva et al. 2011; Boeva et al. 2012) with baseline ploidy = 2, a break-point threshold = 0.8 and
281 coefficient of variation = 0.5 (Scopel et al. 2021). We further optimized the CNV detection by limiting the
282 expected GC content to between 0.35 and 0.55. Variants were further filtered to only include copy
283 number calls that were statistically significant ($p<0.05$) using Wilcoxon Rank Sum Test and a Kolmogorov
284 Smirnov Test. Two metrics of CNVs were assessed for differences across time and between populations:
285 CNV load and the fraction of the genome altered. CNV mutational load is the number of CNV events
286 (amplification or deletion) detected within a population. The fraction of genome altered incorporates
287 the size of each CNV event to determine the amount of the genome that is altered by CNVs. We also
288 differentiated between small (<10kb) and large (>10kb) CNVs. Chromosomes were further considered
289 aneuploid if >60% of the chromosome was identified as amplified or lost.
290
291 ***Calculating population differentiation (F_{st}) and genome similarity (Jaccard index)***
292 We calculated pairwise F_{st} between all divergent- and parallel-evolving parental populations at each of
293 the sampled timepoints, based on single nucleotide polymorphisms (SNPs). We first combined the vcf
294 files generated from freebayes using bcftools v1.19 (Danecek et al. 2011), with parallelization of file
295 compression by gnuparallel v20230422 (Tange 2011), using the default parameters of bcftools merge
296 and the R package poolfstats v2.2.0 (Gautier et al. 2022) on R v3.4 (R Core Team 2023). First the vcf files
297 were converted to pooldata objects, using vcf2pooldata with the default parameters. F_{st} was then
298 calculated using pairwiseFST with the nsnp.per.bjack.block = 150 to calculate the Block-Jackknife
299 estimation of standard error, using an ANOVA framework (Hivert et al. 2018). Similarities between copy
300 number variation calls in different populations and through time were assessed based on the Jaccard
301 similarity coefficient using CNVmetrics R package v3.20 (Belleau et al. 2021; Deschênes et al. 2022).
302

303 **Results**

304 We experimentally evolved yeast populations for 1000 generations in divergent and parallel
305 environments. The four selection environments were media containing either salt, ethanol, or two
306 different concentrations of lithium acetate. These media significantly differ in how much they reduced
307 the fitness of the founder populations, and we have previously provided phenotypic and genetic evidence
308 that these populations become differentially adapted to these environments (Ament-Velásquez et al.
309 2022). At regular time points during experimental evolution, we made crosses between the parallel- and
310 divergent-evolving populations (the 'parents') to measure postzygotic reproductive isolation (F1 spore
311 viability) and used whole population genome sequencing to assess their mutational load, i.e. the number
312 and types of structural variation, and other genomic features of the parent, F1, and F2 hybrids.

313

314 ***Parental phenotypic divergence***

315 We phenotypically profiled the evolving parent populations by measuring their growth capacity (yield) in
316 90 different environments, at increasing times of divergence, using the Scan-o-Matic system for high-
317 throughput microbial phenotyping. These 90 non-selection environments contained the same medium
318 (SC) as the selective environments we used for experimental evolution, but they also each contained an
319 additional growth limiting substance (Table S2). Any phenotypic divergence detected between
320 populations is likely a conservative estimate, as multivariate phenotypes were measured in non-
321 selection environments, and no other traits than growth yield were considered. Also note that we only
322 assessed the phenotypic divergence of evolving parent populations here (not the F1 or F2 crosses), to
323 test for and illustrate their adaptation to the four selection environments due to divergent ecological
324 selection.

325 As expected, with increasing generations of experiment evolution in different environments,
326 divergent-selected parent populations significantly diverged in phenotype, i.e. their yield differed

327 significantly (regression across all divergent-evolved populations: R = 0.14, p = 0.007; **Figure 2A**). In
328 contrast, parent populations evolving in parallel in the same environment did not diverge phenotypically
329 (R = 9.34e-04, p = 0.81; **Figure 2B**). This suggests that the phenotypic divergence of populations evolving
330 under different selection pressures was caused by ecological differences between the four selection
331 environments.
332

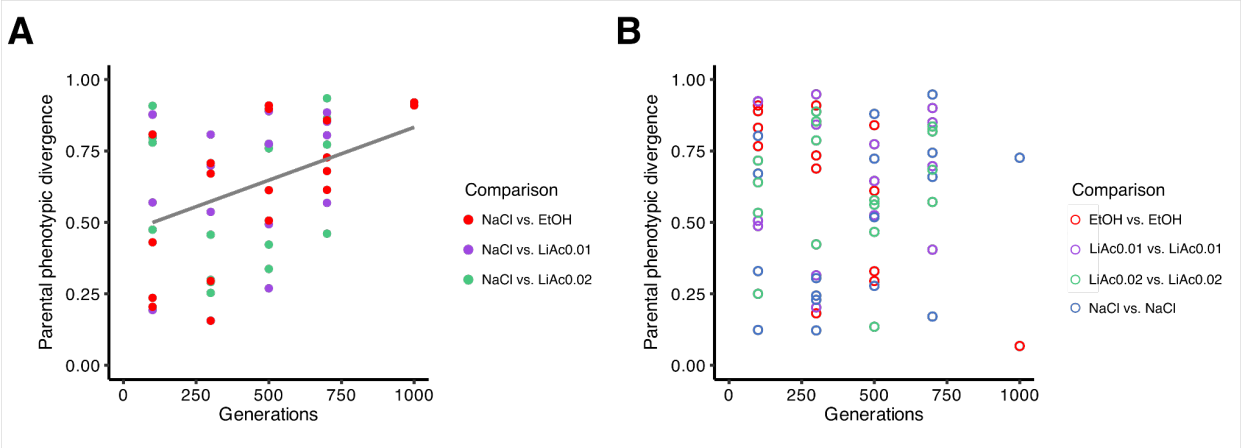

333
334 **Figure 2**: **Phenotypic divergence of evolving parental populations.** Regression of parental phenotypic
335 divergence (the proportion of 90 environments, in which populations significantly differed in yield)
336 against the increasing time (in number of generations) that parental population evolved in the
337 experiment. **A)** Comparisons between divergent-evolved populations in different environments. **B)**
338 Comparisons between parallel-evolved populations in the same environment.
339

340 ***Genetic population differentiation***

341 When comparing parental populations, genetic population differentiation (genome-wide F_{st}) was
342 generally larger (mean = 0.25) in pairwise comparisons between divergent-selected (grey boxes in **Figure**
343 **3A**) than between parallel-selected populations (mean = 0.19, colored boxes). The only exception were
344 comparisons between parallel-selected LiAc0.01 populations (purple boxes), which produced slightly
345 higher F_{st}-values but were not significantly larger than the divergent-selected populations. F_{st} -values
346 increased with the number of generations of evolution in divergent environments (**Figure 3A**, Figure S1),
347 except for comparisons between divergent-selected NaCl and LiAc0.02 populations, which tended to
348 decrease in F_{st} over time. Consistent with their lower F_{st} -values overall, the genomes of parallel-selected

349 populations remained significantly more similar (using the Jaccard similarity index) than the genomes of

350 divergent-selected populations (gray boxes in **Figure 3B**). Together, this suggests that the larger genetic

351 divergence of populations evolving under different selection pressures was caused by ecological

352 differences between the four selection environments.

353

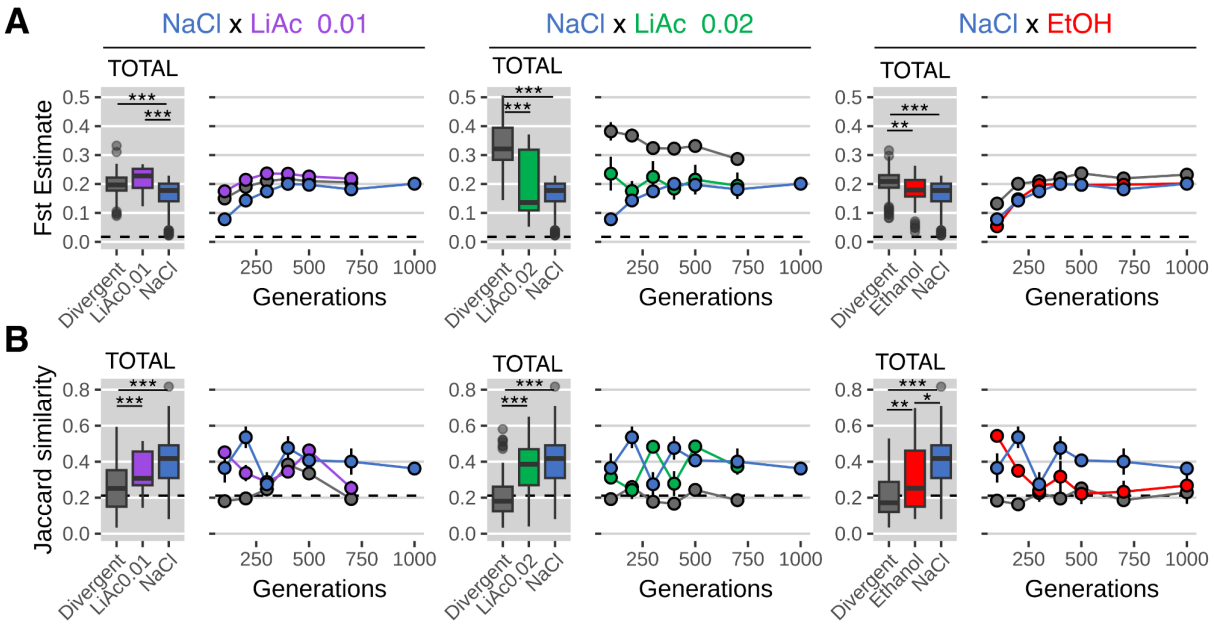

354
355 **Figure 3: Parental genomic population differentiation**. **A)** Genetic population divergence (F_{st}) against
356 the number of parental generations in experimental evolution. Boxplots indicate the first and third
357 quartiles with whiskers extending to the furthest point not exceeding 1.5 x the interquartile range and
358 outliers beyond this are shown as dots. The solid line indicates the median value. **B)** Genomic similarity
359 (Jaccard similarity index) against the number of generations. Box plots show means (thick horizontal
360 line) across all generations of each population type. Circles indicate the mean measurement and the
361 vertical line indicates the standard error of the mean. 'Divergent' indicates comparisons between
362 divergent-selected populations. Asterisks indicate statistical significance using Kruskal-Wallis and
363 pairwise Wilcoxon post hoc tests with Bonferroni corrections (adjusted p-values < 0.001 = ***, < 0.01 =
364 **, < 0.05 = *). Dashed horizontal lines indicate the measured differentiation between the founder
365 populations at the beginning of evolution.
366

367 ***F2 hybrid viability***

368 To measure reproductive isolation, we mated pairs of strains evolving in different environments

369 (divergent selection) or the same environments (parallel selection) to generate F1 hybrids. We then

370 sporulated these to produce F1 spores (gametes), which are their recombined, haploid F2 offspring. We

371 then measured their viability as the fraction of gametes capable of germination and cell colony
372 formation as a measure of reproductive isolation between populations. The viability of F1 spores made
373 between divergent-selected populations was significantly lower than the viability of crosses made
374 between parallel-selected populations (Wilcoxon rank sum test with continuity correction across all
375 generations; W = 1395.5, p = 0.046). Analyzing cross types separately, the viability of offspring from
376 parallel-selected populations was significantly higher than the viability of hybrids made from divergent-
377 selected parents in two cross types (Kruskal-Wallis: NaCl x EtOH: $X^2 = 7.6216$, p = 0.022; NaCl x LiAc0.02:
378 $X^2 = 14.209$, p = 0.001). In the NaCl x LiAc0.01 cross type, the viability of crosses made from parallel-
379 selected populations was similar to that of crosses from divergent-selected populations ($X^2 = 5.834$, p =
380 0.054).

381 Following the breakdown of hybrid viability over time, we found that viability between
382 divergent-selected parents was still relatively high at early time points of divergence (on average 89.1%
383 ± 0.02 at 100 generations) but then decreased substantially between 250 and 500 generations to on
384 average 66% ± 0.08 (**Figure 4**, top left panel). On the contrary, the viability of crosses between parallel-
385 selected populations stayed high throughout the duration of experimental evolution. One exception
386 were the crosses made from parallel-selected populations in LiAc0.02, which dropped in viability after
387 500 generations, to a similar extent as the divergent-selected NaCl x LiAc0.02 hybrids. We discuss
388 potential explanations for this below.

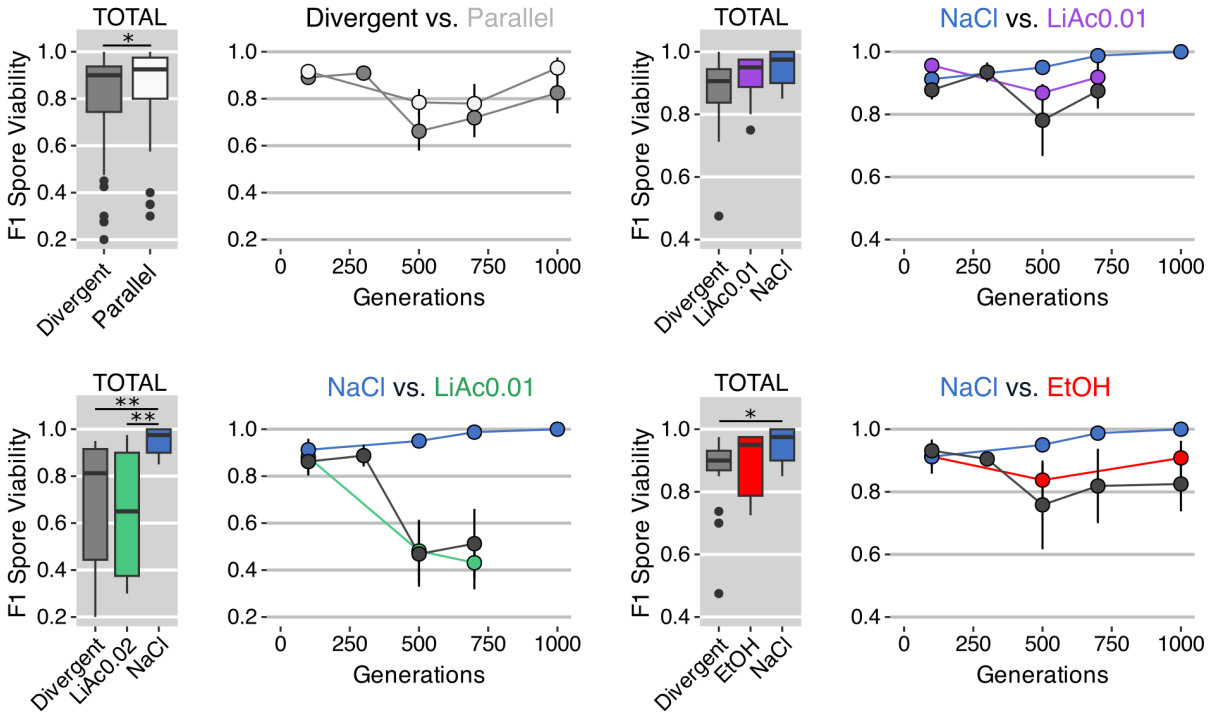

Figure 4: Analysis of reproductive isolation. The viability of F1 spores (i.e. the recombined haploid F2 offspring), which is an inverse measure of reproductive isolation, against the number of parental generations in experimental evolution. Circles indicate the mean measurement and the vertical line indicates the standard error of the mean. Crosses made between parallel-selected populations evolving in the same environment are coloured (or white in the TOTAL plot), crosses made between divergent-selected populations, evolving in different environments, are grey. Box plots show means (thick horizontal line) across all generations of each cross type. 'Divergent' are the crosses between divergent-selected populations (NaCl vs LiAc0.01, NaCl vs LiAc0.02, NaCl vs EtOH). Asterisks indicate statistical significance using Kruskal-Wallis and pairwise Wilcoxon post hoc tests with Bonferroni corrections (adjusted p-values < 0.001 = ***, < 0.01 = **, < 0.05 = *).

The genome-wide mutational landscape of adaptation and hybridization

In an effort to find the genetic mechanisms potentially underlying postzygotic reproductive isolation, we assessed the genome-wide mutational landscape of the divergent-evolved parental populations, and the F1 and F2 hybrid crosses made between them, through all sampled timepoints. We focused on three major mutational classes: single nucleotide variants (SNVs), large structural variants (SVs), and copy number variants (CNVs).

408 We found that all populations showed reduced SNV mutational diversity compared to the
409 founder population within the first 100 generations of evolution (**Figure 5A**). As expected, most
410 identified mutational variants were single nucleotide variants, fewer were insertions and deletions
411 (indels) (Figure S2). The mutational SNV load in LiAc0.02 populations was consistently lower than in
412 populations evolving in NaCl and in their F1 and F2 hybrids, and remained low through time (Kruskal-
413 Wallis: $X^2 = 44.95$, $p < 0.001$, **Figure 5A**). This pattern remained after filtering for mutational variants
414 estimated by SnpEff to have high impact (Kruskal-Wallis: $X^2 = 13.07$, $p=0.004$, **Figure 5C**, Figure S3).
415 LiAc0.02 populations also showed a lower SNV mutational load than the populations evolving in the
416 weaker concentration of lithium acetate (LiAc0.01). It is possible that this is the result of stronger
417 purifying selection in LiAc0.02 populations from the start. But since populations evolving in the stronger
418 concentration of lithium acetate have likely also undergone fewer mitotic generations, this may also
419 reflect mutations accumulating primarily as a function of reproductive time. In the other three parental
420 population types (NaCl, LiAc0.01 and EtOH), SNV mutational load decreased over time (**Figure 5B**) and
421 the pattern stayed consistent when filtering for only mutations with high impact on fitness (Figure S3A).
422 Conversely, in the F1 ($R = 0.48$, $p < 0.01$, in grey) and F2 hybrid populations ($R = 0.57$, $p < 0.01$, in yellow),
423 we found a total increase in mutational load over time (**Figure 5B**). Thus, the more the parental
424 populations diverged phenotypically and genetically over time, the more single nucleotide mutational
425 variants were detected in their resulting F1 and F2 hybrid populations.

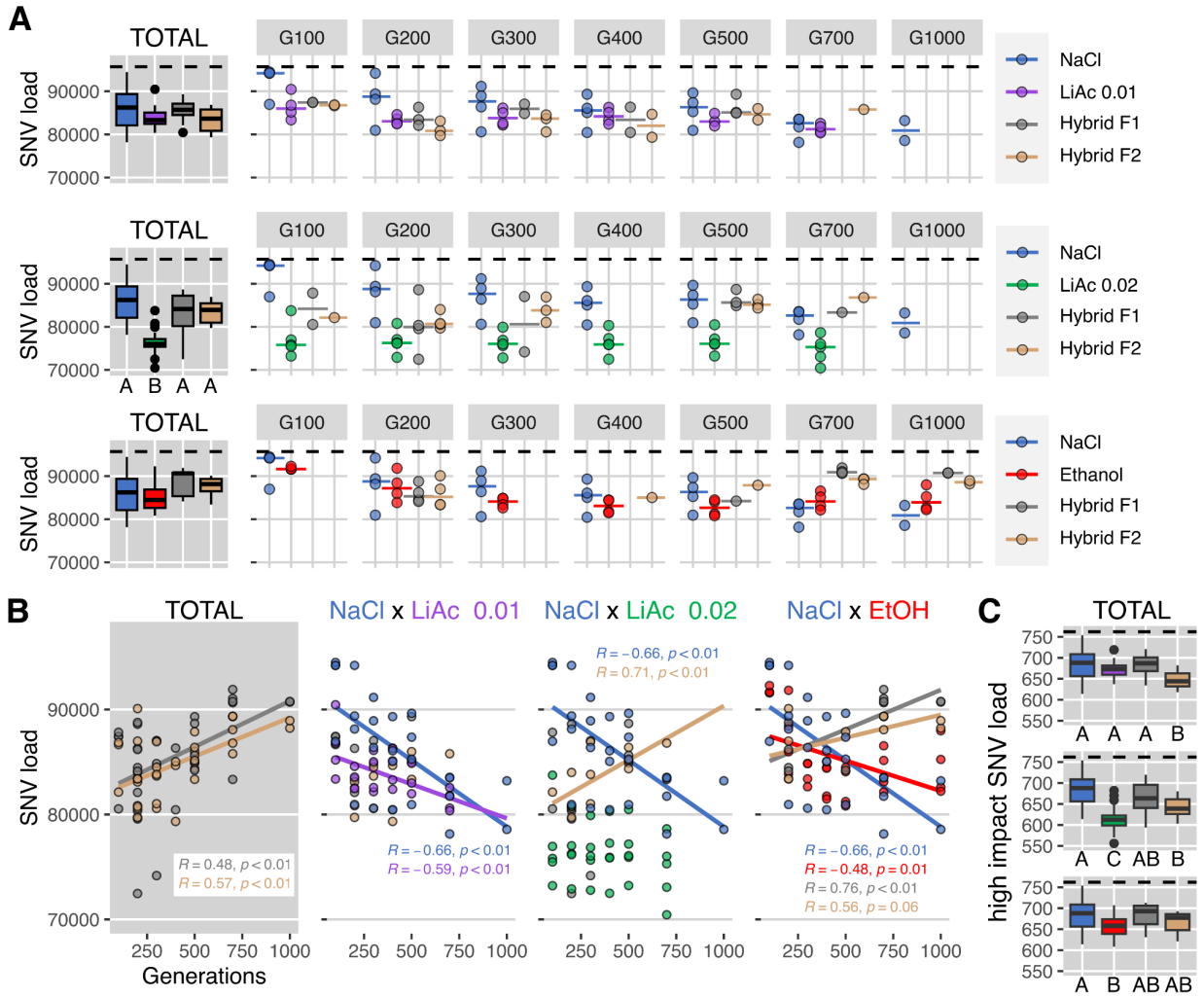

Figure 5: The single nucleotide variant mutational landscape of hybridization. A) The SNV mutational load consists of the number of mutational variants and indels (insertions and deletions) within a population. The median SNV mutational load of populations is indicated by the colored solid line. Gray plots show mutational load averaged across all sampled timepoints (TOTAL) for the three types of hybrid crosses. Other plots show data from crosses made at 7 timepoints of increasing parental divergence (number of generations). The mean mutational load of the founder population is indicated by the dashed black line. Boxplots indicate the first and third quartiles with whiskers extending to the furthest point not exceeding 1.5 x the interquartile range and outliers beyond this are shown as dots. The solid line indicates the median value. Letters indicate statistical significance using Kruskal-Wallis and pairwise Wilcoxon post hoc tests with Bonferroni corrections. **B)** Linear regression (Pearson R) between SNV mutational load and increasing timepoints of parental divergence (number of generations). Only significant linear relationships are shown. The gray plot includes F1 and F2 hybrids across all crosses. **C)** SNV mutational load after filtering for high impact mutations on gene function using SnpEff v5.2 (Cingolani et al. 2012). The mutational load is averaged across all timepoints (TOTAL) for each hybrid cross. The mean mutational load of the founder population is indicated by the dashed black line.

443 Different letters (A, B and C) indicate statistically significant differences using Kruskal-Wallis and pairwise
444 Wilcoxon post hoc tests with Bonferroni corrections.
445

446 Analysis of structural variants (i.e. insertions, deletions, duplications, inversions and
447 interchromosomal translocations that are > 8bp) showed that the total number of SVs found in the
448 evolving parental populations remained comparable to the levels in the founder population (**Figure 6A**).
449 Unlike the pattern we saw in SNV mutational load, the number of SVs harbored in parental populations
450 increased over time (**Figure 6C**). This positive linear relationship was consistent for populations evolving
451 in NaCl ($R = 0.72$, $p < 0.01$), LiAc0.01 ($R = 0.6$, $p < 0.01$) and LiAc0.02 ($R = 0.61$, $p < 0.01$), but not for EtOH
452 populations, which already had elevated levels of SVs ($p < 0.001$) early on but then decreased over time
453 ($R = -0.7$, $p < 0.01$; **Figure 6A**).
454 Strikingly, we found very high levels of SVs in all types of F2 hybrid crosses, right from the
455 beginning of parental population divergence (Kruskal-Wallis: NaCl x LiAc0.01: $X^2 = 22.87$, $p < 0.001$; NaCl
456 x LiAc0.02: $X^2 = 30.28$, $p < 0.001$; NaCl x EtOH: $X^2 = 34.45$, $p < 0.001$). In most cases, F2 hybrid populations
457 harboured almost twice as many structural variants compared to the corresponding parental
458 populations and the F1 hybrids. This pattern was seen across SV types collectively, but was particularly
459 prominent for insertions, deletions and interchromosomal translocations (breakend mutations, **Figure**
460 **6B**, Figure S4-S8). Duplications were rare compared to deletions and insertions and are therefore not
461 driving the elevated levels of SVs observed in F2 hybrid genomes (**Figure 6B)**. Because F2 hybrids are
462 distinguished from F1 hybrids and the parent populations only by having passed through one round of
463 meiosis, the additional load of structural variants we found in F2 hybrids likely arose due to meiotic
464 errors.
465

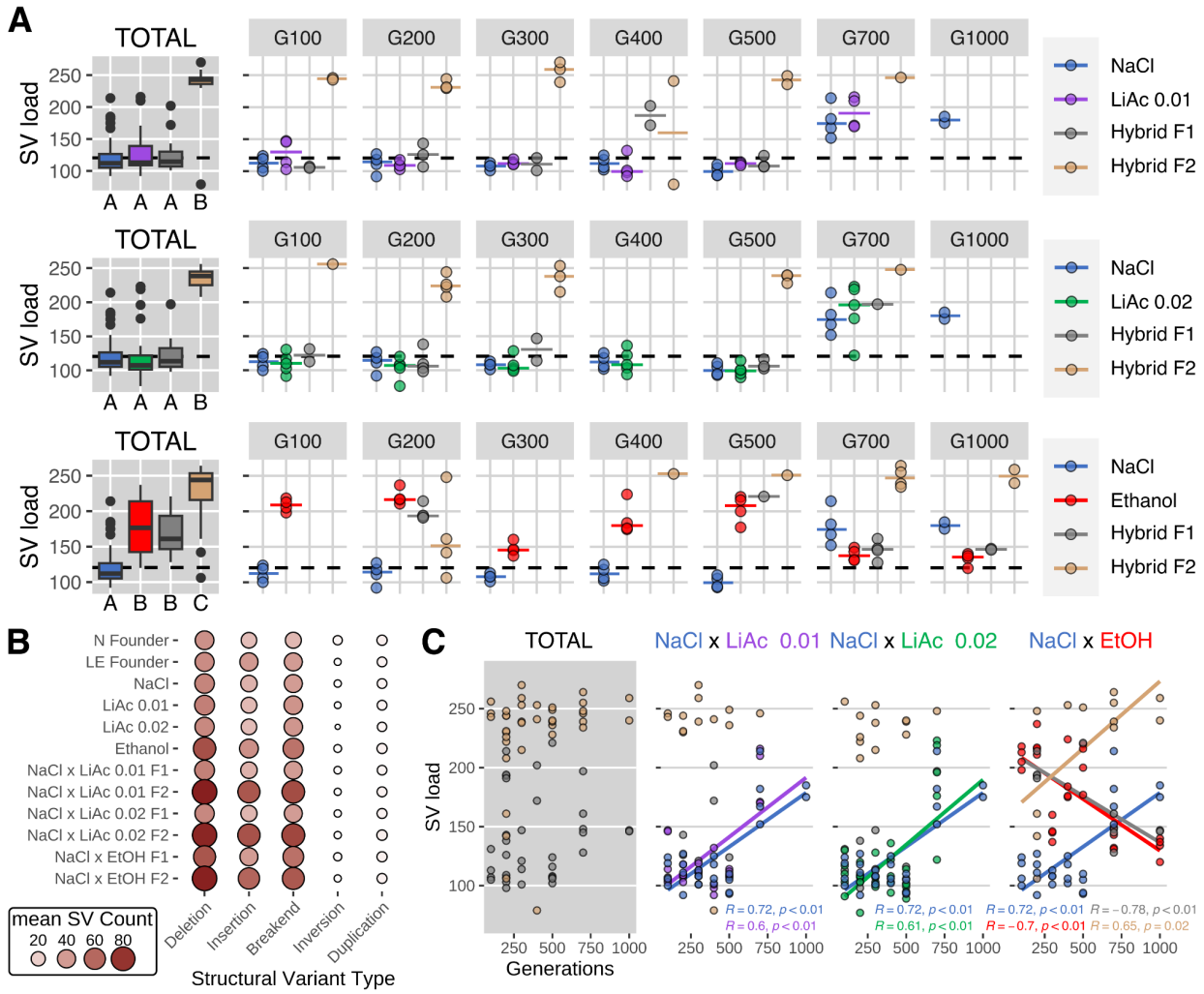

Figure 6: The structural variant mutational landscape of hybridization. A) Structural variant (SV) mutational load consists of the number of deletions, insertions, inversions, tandem duplications and interchromosomal translocations (> 8bp) detected in the population. Gray plots show SV mutational load averaged across all sampled timepoints (TOTAL) for the three types of hybrid crosses. Other plots show data from crosses made at 7 timepoints of increasing parental divergence (number of generations). The mean mutational load of the founder population is indicated by the dashed black line. Boxplots indicate the first and third quartiles with whiskers extending to the furthest point not exceeding 1.5 x the interquartile range and outliers beyond this are shown as dots. The solid line indicates the median value. Different letters (A, B and C) indicate statistically significant differences using Kruskal-Wallis and pairwise Wilcoxon post hoc tests with Bonferroni corrections. **B)** Mean structural variant count of each type of structural variant (deletion, insertion, breakend, inversion and duplication) for each environment and cross. Node color and size indicates the mean count of each variant type across all timepoints. **C)** Linear regression (Pearson R) between SV mutational load and increasing timepoints of parental divergence (number of generations). Only significant linear relationships are shown. The gray plot includes F1 and F2 hybrids from all crosses.

483

484 In addition to structural variants, we also more comprehensively assessed copy number
485 variations (CNV) across the genome, which are a subtype of structural variation. In the structural
486 variation analysis, detection of variants was limited by the read pair fragment size. However, copy
487 number variants can range from small focal amplifications or deletions to chromosome arm, or whole
488 chromosome aneuploidies. Therefore, we used an approach that employs sequencing read depth and
489 allelic imbalances to estimate segmented copy number uniformly throughout the genome. On average,
490 parental populations, F1 and F2 hybrids had a lower CNV mutational load compared to the founder
491 population (dashed black lines in **Figure 7A**). This pattern remained consistent when including the size of
492 each copy number variant to estimate the fraction of altered genome content (**Figure 7B**). Most
493 populations showed moderate levels (< 10%) of total alteration (amplification + deletion) of the genome
494 by CNV (**Figure 7B**). However, NaCl populations had a larger fraction of their genomes altered in copy
495 number than parental populations evolved in LiAc and EtOH (pairwise Wilcoxon test: vs LiAc0.01: p
496 <0.001; vs LiAc0.02: $p <0.001$; vs EtOH: $p =0.012$), mainly due to a large fraction of the genome
497 alterations (> 20%) in three parallel-evolved NaCl populations at three different time points.

498 Strikingly, the F2 hybrid genomes of all three crosses contained significantly fewer CNVs than
499 parental populations and most F1 hybrids (**Figure 7A**; Kruskal-Wallis: NaCl x LiAc0.01: $X^2 = 30.1$, $p <$
500 0.001; NaCl x LiAc0.02: $X^2 = 24.4$, $p < 0.001$; NaCl x EtOH: $X^2 = 37.7$, $p < 0.001$) and F2 hybrid genomes of
501 all crosses were significantly less altered by CNVs (in % genome) than the parental populations (**Figure**
502 **7B**). Overall, we found that amplifications were more common than deletions across populations and
503 through time (Figure S9). Similar to SNVs and SVs, we found consistent patterns of linear increase or
504 decrease in CNVs with the number of parental generations of evolution in divergent environments
505 (**Figure 7C**). In the parental NaCl ($R = -0.59$, $p < 0.01$) and LiAc0.02 ($R = -0.56$, $p < 0.01$) populations, the
506 CNV mutational load decreased with the number of generations. In the LiAc0.01 parents, the same

507 pattern was seen but was not significant (R = -0.37, p = 0.08). Interestingly, CNV mutational load was
508 often relatively stable until approximately 500 generations, followed by a steep decrease (**Figure 7A,**
509 **7C**). In the EtOH parents, we found the opposite pattern, with CNV load increasing with the number of
510 generations (R=0.72, p <0.01), affecting the F1 hybrid genomes between NaCl and EtOH in the same way
511 (R = 0.73, p = 0.01).

512 Lastly, we sought to understand if these patterns of CNV load were driven by small focal variants
513 or larger multi-kilobase alterations, including whole chromosomal aneuploidies. We found that, as
514 expected, the majority of variants were small (< 10kb) and contributed significantly to the global pattern
515 found in CNV load (compare upper row of plots in **Figure 7D** to **Figure 7A**). A closer examination of the
516 number of larger alterations (> 10kb; middle row of plots in **Figure 7D)** revealed that the F2 hybrid
517 genomes of two hybrid crosses (NaCl x LiAc0.01, NaCl x LiAc0.02), showed significantly fewer large
518 alterations (on average 12.1) than their respective parents (on average 20.8) and F1 hybrids (on average
519 19.4). This pattern is further emphasized when examining exclusively the number of aneuploid
520 chromosomes (>60% amplified or deleted) found in each sample (lower row of plots in **Figure 7D**). On
521 average, F2 hybrid genomes carried fewer aneuploidies (mean=0.24 chromosomes) compared to parent
522 (mean=0.67) and F1 hybrid genomes (mean=0.64).

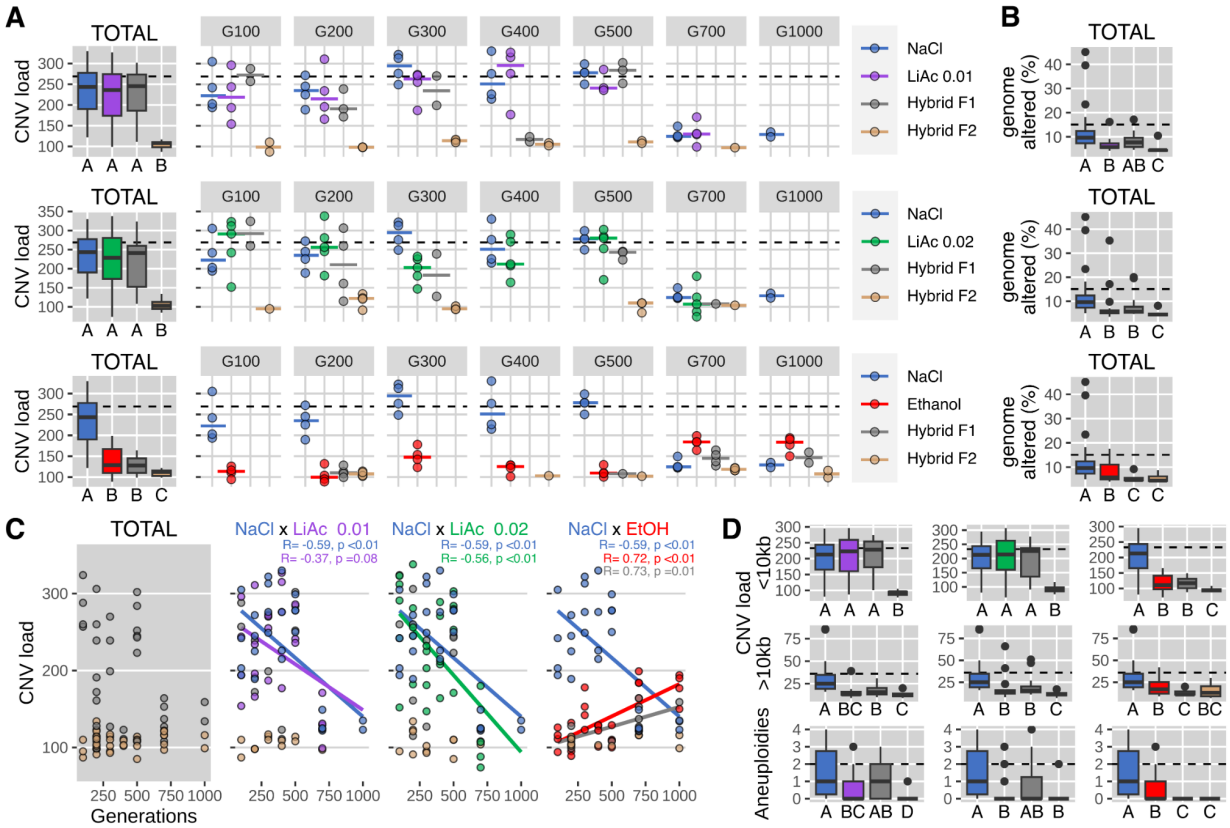

Figure 7: The copy number variant mutational landscape of hybridization. A) Copy number variant (CNV) mutational load consisting of amplifications, deletions and aneuploidies. Gray plots show CNV mutational load averaged across all sampled timepoints (TOTAL) for the three types of hybrid crosses. Other plots show data from crosses made at 7 timepoints of increasing parental divergence (number of generations). The mean mutational load of the founder population is indicated by the dashed black line. Boxplots indicate the first and third quartiles with whiskers extending to the furthest point not exceeding 1.5 x the interquartile range and outliers beyond this are shown as dots. The solid line indicates the median value. Different letters (A, B and C) indicate statistically significant differences using Kruskal-Wallis and pairwise Wilcoxon post hoc tests with Bonferroni corrections. **B)** The fraction of the genome altered (%) across all sampled timepoints (TOTAL) for the three types of hybrid crosses. Colors, boxplots and statistical significance are consistent with panel A. **C)** Linear regression (Pearson R) between CNV mutational load and increasing timepoints of parental divergence (number of generations). Only significant linear relationships are shown. The gray plot includes F1 and F2 hybrids from all crosses. **D)** The distribution of large (>10kb) CNVs, small (<10kb) CNVs and chromosome aneuploidy (>60% amplified or deleted) across all sampled timepoints for the three types of hybrid crosses. Colors, boxplots and statistical significance are consistent with panel A.

The distribution of mutational events across the genome

After assessing the genome-wide mutational landscape in terms of SNVs, SVs, and CNV mutational load, we determined the distribution of these mutational events across the genome. We found that the rate

544 of SNVs was not uniformly distributed, but instead showed chromosomal biases (Kruskal-Wallis: X^2 =
545 147.28, p <0.001, **Figure 8A**). Chromosomes VI and VIII had significantly higher frequencies of SNVs (16.7
546 and 14.1 mutations/kb, respectively). Chromosome I and IX also showed slightly elevated SNV
547 frequencies (10.8 and 9.35 mutations/kb, respectively). Chromosome VII on the other hand showed a
548 significantly lower frequency of SNVs (2.29 mutations/kb). The remaining chromosomes had
549 approximately equal frequencies of SNVs (6.39-7.34 mutations/kb). These chromosomal biases in SNV
550 distribution already existed in the founder population and remained consistent across all parental
551 lineages and all F1 and F2 hybrids (**Figure 8A**).

552 The distribution of structural variant (SV) events were also not uniformly distributed throughout
553 the genome (Kruskal-Wallis: X^2 = 60.06, p <0.001, **Figure 8B**). Similar to the SNV distribution, we found
554 highly elevated rates of SVs on chromosome VI (0.03 mutations/kb). We also found peaks in the rate of
555 SVs in chromosomes I, III, and IX in most parental and hybrid populations.

556 The proportion of whole chromosomes altered by copy number variants was not consistent
557 across environments and hybrid crosses (**Figure 8C**). Interestingly, F2 hybrids of all crosses showed the
558 lowest levels of copy number alterations, and aneuploidy (defined as > 60% of chromosome
559 amplification) was consistently rare across all F2 hybrid chromosomes. We discuss the implications of
560 the near absence of aneuploidies and large genome alterations in F2 hybrid genomes below. Our
561 analysis shows that the two founding populations each carried aneuploid chromosomes. The NaCl
562 founder population (N founder, **Figure 8C**) had an extra chromosome X, while the LE founder population
563 had three aneuploid chromosomes (I, III and VI). Parental NaCl populations subsequently lost the extra
564 chromosome X over the course of experimental evolution, but evolved an aneuploid chromosome I and
565 underwent alterations of large portions of chromosome III and VI. Chromosome I was also heavily
566 altered in parent populations evolving in LiAc 0.01 (40%), LiAc 0.02 (37%), and EtOH (25%). Similarly, F1
567 hybrid crosses between NaCl and the two LiAc populations (to a lesser extent the NaCl x EtOH F1

568 hybrids) also showed large copy number alterations in chromosomes I, III, and VI (**Figure 8C**). Confirming
569 our previous result (Ament-Velásquez et al. 2022), we also recovered a chromosome X aneuploidy in
570 two parental EtOH populations and the chromosome XI aneuploidy in one parental EtOH population
571 here.

572 The 16 chromosomes of *S. cerevisiae* range widely in size from 270kb (chrVI) to 1,531kb (chrIV;
573 **Figure 8D**). As might be expected, larger chromosomes are larger targets for SNVs, SVs and CNVs and
574 therefore have higher overall mutational load for each mutational class. Even after correcting
575 mutational load for chromosome size, either by reporting SNVs and SVs as mutations per kilobase or
576 reporting CNVs as the percentage of chromosome altered, we still found a strong negative relationship
577 between chromosome size and SNV, SV and CNV mutational rate (**Figure 8D**). Smaller chromosomes had
578 elevated rates of mutation while larger chromosomes were rarely affected. This pattern is most striking
579 in CNVs where, as previously mentioned, chromosomes I, III and VI were disproportionately altered. This
580 is interesting because chromosomes I, III, and VI are the smallest chromosomes in the yeast genome and
581 have been frequently reported to carry aneuploidies in other yeast studies as well (reviewed in Gilchrist
582 and Stelkens 2019), likely because aneuploidies of smaller chromosomes cause fewer deleterious gene
583 dosage effects and can be compensated for at the proteome level (Muenzner et al. 2024). This pattern
584 of chromosome size bias for CNVs extends beyond intraspecific crosses and has been found across
585 interspecific yeast hybrids with diverse ancestries (Bendixsen et al. 2021).

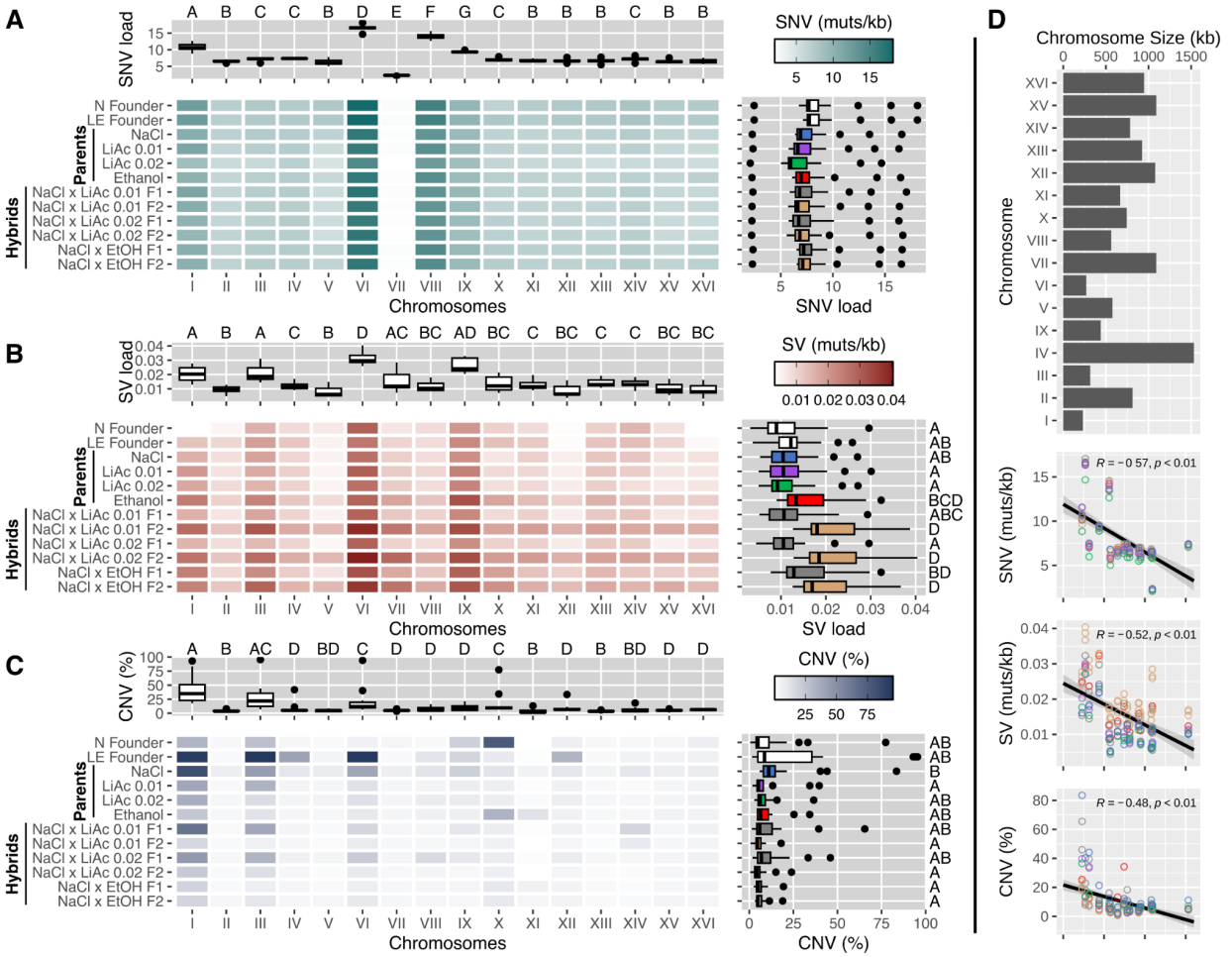

Figure 8: The distribution of mutational events across the genome. A) The mean number of events (mutations/kb) for each chromosome across all available timepoints. The top graph shows the distribution of mean SNV counts for each chromosome, while the right graph shows the distribution for each environment and hybrid cross. Boxplots indicate the first and third quartiles with whiskers extending to the furthest point not exceeding 1.5 x the interquartile range and outliers beyond this are shown as dots. The solid line indicates the median value. Different letters (A, B, C, D) indicate statistically significant differences using Kruskal-Wallis and pairwise Wilcoxon post hoc tests with Bonferroni corrections. **B)** The mean number of structural variant (SV) events (mutations/kb). **C)** The mean amount of genome altered (%) by copy number variants (losses and gains), including whole chromosome aneuploidies. **D)** The relationship between chromosome size and SNVs, SVs or CNVs. The barplot indicates the size of each of the 16 chromosomes in *Saccharomyces cerevisiae* reported in kilobases. The linear correlations show the mean SNV (muts/kb), SV (muts/kb) or CNV (% genome altered) for each population and for each chromosome as shown in the top graphs of panels A, B and C. The colors of each node indicate the populations (NaCl, LiAc0.01, LiAc0.02, EtOH, Hybrid F1, Hybrid F2).

601

602 **Discussion**

603 We used experimental evolution with budding yeast to test for the evolution of reproductive isolation as
604 a result of ecologically divergent selection, a process called ecological speciation (Mayr 1947; Schluter
605 2001; McKinnon et al. 2004; Nosil 2012; Jarrett et al. 2024). Previous studies with yeast have tested for
606 reproductive isolation between species that have diverged millions of years ago, which translates into
607 billions of generations (Greig et al. 2002; Shapira et al. 2014; Stelkens et al. 2014; Bernardes et al. 2017;
608 Eberlein et al. 2019; Gallone et al. 2019; Zhang et al. 2020; Bautista et al. 2021; Brice et al. 2021;
609 Bautista et al. 2023). Here, instead of starting with already divergent species, separated by billions of
610 generations, each with a complex evolutionary history of selection, genetic drift, recombination, and
611 gene flow, we generated phenotypic and genetic divergence over only a few hundred generations. We
612 evolved replicate populations in allopatry, in four different environments, under both ecologically
613 divergent and parallel selection. Hence, we controlled the type and degree of selection, minimized
614 genetic drift and recombination, and excluded gene flow. We systematically produced hybrid crosses
615 between these populations at seven time points of experimental evolution, to test whether
616 reproductive isolation evolved between the divergent-selected populations, as predicted by ecological
617 speciation theory.

618 First, we confirmed that populations when evolved in different environments, increasingly
619 diverged in phenotypic traits that were not directly under selection. The parallel-selected (control)
620 populations on the other hand remained phenotypically similar (**Figure 2**). This provides evidence for
621 large scale phenotypic differentiation under divergent selection. Second, the genomes of divergent-
622 selected populations became more genetically differentiated over time, showing higher F_{st} - values and
623 lower similarity (Jaccard index) than those of the parallel-selected populations (**Figure 3**). Third, we
624 found that divergent-selected populations produced hybrid gametes with reduced viability, which is a

625 classic signature of postzygotic reproductive isolation in the form of hybrid breakdown (**Figure 4**).
626 Zygotes generated from parallel-selected populations on the other hand remained reproductively
627 compatible (**Figure 4**). Together, our results suggest that partial reproductive isolation evolved due to
628 divergent ecological selection in our experiment. Alternative processes, such as mutation-order effects
629 (Schluter 2009; Ono et al. 2017), may have contributed to the build up of reproductive barriers, but
630 since most parallel-selected populations remained compatible, neither the timing nor the order in which
631 mutations occurred likely played a large role.

632 Early experiments, e.g. in fruit flies with similar set-ups of divergent- and parallel-selected lines
633 on different media (Dodd 1989) and a large body of theory (reviewed in Kirkpatrick and Ravigné 2002)
634 have demonstrated the evolution of reproductive isolation as a consequence of adaptive divergence
635 (Nosil 2012). Here, we have taken additional steps to understand the genetic basis of this hybrid
636 breakdown. Our population genomic analyses show that, as parental populations diverged
637 phenotypically and genetically over time, the mutational load of single nucleotide variants (SNVs)
638 steadily increased in F1 and F2 hybrids (**Figure 5)**, with a bias for chromosomes I, VI, and VIII (**Figure 8A**).
639 This may point to increasingly defective DNA repair pathways in hybrid genomes. But even more
640 strikingly, F2 hybrid populations harboured more than twice as many structural variants (SVs) than their
641 respective parental populations and the F1 hybrids. This pattern was seen across all SV types (**Figure 6**),
642 but was particularly strong for insertions, deletions, and interchromosomal translocations (breakend
643 mutations, Figure S4-S8) with strong chromosomal biases for chromosomes I, III, VI, and IX (**Figure 8B**).
644 Because F2 hybrids differ from F1 hybrids only by one meiotic event (and a few mitotic generations
645 before and after sporulation that are negligible), the increase in structural variants seen in F2 hybrids
646 can only reasonably be explained by errors during meiosis. This suggests that ecological divergence has
647 led to hybrid offspring with higher genomic instability due to meiotic recombination errors (e.g. unequal
648 or incorrect crossing overs), resulting in frequent chromosomal rearrangements (SVs).

649 Interestingly, F2 hybrids showed the lowest levels of copy number alterations, and aneuploidy
650 rates were consistently low across all chromosomes in F2 hybrid genomes (**Figure 7, Figure 8C**). This is
651 surprising, because in contrast to the high SV load found in hybrid genomes (**Figure 6**), errors during
652 meiosis seem to not have led to a detectable increase in chromosome non-disjunction and aneuploidy.
653 Meanwhile, all parent and F1 hybrid populations contained various aneuploidies, especially in
654 chromosomes I, III, and VI, which are the smallest chromosomes in the yeast genome and frequently
655 reported to carry aneuploidies (reviewed in (Gilchrist and Stelkens 2019). A plausible explanation for the
656 surprising absence of aneuploidies in F2 hybrids is that, by default, we only sequenced viable genotypes
657 that had successfully passed through meiosis and germinated. Average mortality due to lethal
658 aneuploidies is likely high in the recombined haploid gametes, where copy number imbalances imposed
659 by aneuploidies are more pronounced, and lethality has additional opportunities to manifest when
660 strains are pushed through germination. As a result, aneuploidies may have been efficiently purged from
661 F2 hybrid genomes before the sequencing stage.
662 Experimental and genetic work in interspecific yeast crosses, made from species separated by
663 billions of generations and high nucleotide divergence (>10%), has shown that the main reason for
664 hybrid breakdown in yeast is antirecombination (Hunter et al. 1996; Rogers et al. 2018; Bozdag et al.
665 2021). Antirecombination suppresses crossovers during meiosis when nucleotide divergence along
666 chromosomes is too high. The ensuing mispairing of homologous chromosomes causes missegregation
667 into the hybrid gametes, leading to lethal aneuploidies and typically > 90% spore mortality in
668 interspecific yeast crosses. This process has also been shown to cause hybrid sterility in mice, where it is
669 controlled by the Prdm9 gene (Forejt and Jansa 2023). However, antirecombination due to genome-
670 wide nucleotide divergence is unlikely to have played a role in the hybrid breakdown we observed here,
671 given the short evolutionary time span of our experiment. Instead, we suggest that the following
672 process underlies the build up of reproductive barriers here: First, divergent ecological selection in the

673 parent populations has led to SVs with positive (adaptive) fitness effects and additional neutral SVs
674 hitchhiking along with them. These parental SVs then interfered with hybrid meiosis, causing additional
675 SVs to emerge in the hybrid genomes, due to unequal or incorrect crossing over. Cumulatively, the high
676 SV load of the hybrid genomes then negatively affected gamete viability, germination, and colony
677 formation, disrupting cell function and homeostasis (Chang et al. 2013; Liu et al. 2022). In short, we
678 suggest that the most likely genetic mechanism underlying hybrid breakdown in our experiment is the
679 high structural variant load of the hybrid genomes, which was jump-started by the increasing number of
680 SVs accumulating in the divergent-selected parent populations (**Figure 6**).

681 We saw one interesting exception in crosses between parallel-selected LiAc0.02 populations
682 where, against our expectations, gamete viability decreased over time (**Figure 4**). We previously found
683 that three of four replicate populations evolving in LiAc0.02 had turned (functionally) haploid early on in
684 experimental evolution (Ament-Velásquez et al. 2022). In haploid populations, beneficial mutations can
685 sweep to fixation faster and deleterious mutations are more quickly purged by purifying selection, as
686 they are not masked by heterozygosity (Gerstein et al. 2011; Cervantes et al. 2023). These processes are
687 particularly efficient in large populations exposed to stressful environments with strong selection, which
688 the LiAc0.02 environment represents (Ament-Velásquez et al. 2022). Propelled by clonal interference,
689 this may have affected the adaptive dynamics (the rate and direction of allele frequency changes) in the
690 LiAc0.02 populations in idiosyncratic ways, leading to substantial genetic differentiation and
691 incompatibilities between them, despite parallel selection pressures.

692 But what is the genetic architecture of the partial reproductive isolation in our experiment? The
693 pattern of decreasing genomic similarity and increasing F_{st} between divergent-selected populations
694 (while parallel-selected populations remained similar), and the vast genome-wide instability found in
695 hybrid genomes, does suggest that reproductive isolation is based on multiple genomic regions and that
696 'continents' rather than 'islands' of differentiated loci are operating together (Michel et al. 2010).

697 However, due to the absence of sexual recombination during the evolution of the parent populations in
698 our experiment, other evolutionary mechanisms may have also caused large genomic regions to become
699 differentiated. Effects of clonal interference and linked selection for example, i.e. the competition
700 between multiple beneficial mutations arising independently in the same population leading to only one
701 lineage sweeping through the population, may have caused genetic differentiation between populations
702 that is not due to ecological selection alone. Although our previous work has identified the number and
703 types of adaptive mutations segregating and fixing in the evolving parental populations (Ament-
704 Velásquez et al. 2022), our pool-seq approach does not provide haplotype information. Thus, we cannot
705 infer which and how many genes are causing reproductive isolation, how large their effect sizes are, and
706 whether they are genomically clustered (Nosil and Feder 2012). Directed crosses between parents with
707 known genotypes, and dissecting and genotyping a large number of recombined F2 gametes, could
708 identify incompatible chromosomes, chromosomal regions, or individual genes causing reproductive
709 isolation in this system.
710
711 ***Conclusions***
712 Selection against hybrids due to ecological factors, when hybrid phenotypes are ill-adapted to existing
713 ecological niches, has traditionally been considered as being different from selection arising from
714 epistatic (Dobzhansky-Muller) incompatibilities (Thompson et al. 2023). There is a recent push to close
715 this gap between evolutionary ecology and speciation genetics, and to focus more on the role of the
716 environment and ecological adaptation in driving what we traditionally think of as 'intrinsic' genetic
717 isolation barriers (Anderson et al. 2023; Thompson et al. 2023). Our study contributes to bridging this
718 gap by synthesizing phenotypic and whole genome data, and demonstrating that divergent ecological
719 adaptation can indeed promote intrinsic reproductive isolation, consistent with predictions of ecological
720 speciation theory. Our population genomics results show that divergent ecological selection, even for

721 relatively few mitotic generations, can lead to vast genomic instability in F2 hybrids, including deletions,
722 inversions, and interchromosomal translocations. Thus, our multifaceted approach of combining
723 experimental evolution with sexual microbes, hybridization at increasing time points of divergence,
724 high-throughput phenotyping, and comparative genomics, confirms the role of ecology in driving
725 reproductive isolation and speciation. Our approach can be further developed to provide a
726 comprehensive empirical framework to test different concepts in speciation research. This includes, for
727 instance, i) testing if the speciation continuum is a 'continuum of reproductive isolation' (Stankowski
728 and Ravinet 2021), by measuring whether the accumulation of reproductive isolating barriers is gradual
729 over extended evolutionary time frames, ii) testing if the 'speciation hypercube' captures the complexity
730 of species divergence (Dieckmann et al. 2004; Bolnick et al. 2023), by including more phenotypic and
731 genetic variables, and iii) to better understand the evolution of hybrid fitness during speciation by
732 including additional data sets (e.g. gene interaction networks (Dagilis et al. 2019), which could reconcile
733 the contrasting outcomes of epistatic genetic interactions leading to hybrids with both increased
734 (heterosis) and decreased fitness (hybrid inviability) during different stages of speciation.
735

736 **Acknowledgements**

737 We thank Maria de la Paz Celorio Mancera, Viktoria Köppä, and Zebin Zhang for helping with serial
738 transfers and media preparation, and Lorena Ament-Velásquez for bioinformatics advice. Computation
739 was performed on resources provided by SNIC through Uppsala Multidisciplinary Center for Advanced
740 Computational Science (UPPMAX) under Projects NAISS2023/23-519 (Small Storage) and NAISS2023/22-
741 62 and NAISS2023/22-924 (Small Compute). We acknowledge support from Science for Life Laboratory,
742 the National Genomics Infrastructure, NGI, and Uppmax for providing assistance in massive parallel
743 sequencing and computational infrastructure. This work was supported by Swedish Research Council

Project Grants (2022-03427 to R.S. and 2022-03024 to J.W.), a Knut and Alice Wallenberg Foundation Grant (2017.0163 to R.S.), and the Wenner-Gren Foundations (UPD2018-0196, UPD2019-0110 to D.B.).

References

Alalam H, Graf FE, Palm M, Abadikhah M, Zackrisson M, Boström J, Fransson A, Hadjineophytou C, Persson L, Stenberg S, et al. 2020. A High-Throughput Method for Screening for Genes Controlling Bacterial Conjugation of Antibiotic Resistance. *mSystems* 5:e01226-20.

Ament-Velásquez SL, Gilchrist C, Rêgo A, Bendixsen DP, Brice C, Grosse-Sommer JM, Rafati N, Stelkens R. 2022. The Dynamics of Adaptation to Stress from Standing Genetic Variation and de novo Mutations. *Molecular Biology and Evolution* 39:msac242.

Anderson SAS, López-Fernández H, Weir JT. 2023. Ecology and the Origin of Nonephemeral Species. *The American Naturalist* 201:619–638.

Anderson SAS, Weir JT. 2022. The role of divergent ecological adaptation during allopatric speciation in vertebrates. *Science* 378:1214–1218.

Andrews S. 2010. FastQC: A Quality Control tool for High Throughput Sequence Data. Available from: https://www.bioinformatics.babraham.ac.uk/projects/fastqc/

Bautista C, Gagnon-Arsenault I, Utrobina M, Fijarczyk A, Bendixsen DP, Stelkens R, Landry C. 2023. Hybrid adaptation is hampered by Haldane's sieve. *bioRxiv*:2023–12.

Bautista C, Marsit S, Landry CR. 2021. Interspecific hybrids show a reduced adaptive potential under DNA damaging conditions. *Evolutionary Applications* 14:758–769.

Bell G, Gonzalez A. 2011. Adaptation and Evolutionary Rescue in Metapopulations Experiencing Environmental Deterioration. *Science* 332:1327–1330.

Belleau P, Deschênes A, Beyaz S, Tuveson DA, Krasnitz A. 2021. CNVMetrics package: Quantifying similarity between copy number profiles. *F1000Research* [Internet] 10. Available from: https://f1000research.com/slides/10-737

Bendixsen Devin P, Gettle N, Gilchrist C, Zhang Z, Stelkens R. 2021. Genomic Evidence of an Ancient East Asian Divergence Event in Wild Saccharomyces cerevisiae. *Genome Biology and Evolution* 13:evab001.

Bendixsen, Peris D, Stelkens R. 2021. Patterns of Genomic Instability in Interspecific Yeast Hybrids With Diverse Ancestries. *Frontiers in Fungal Biology* [Internet] 2. Available from: https://www.frontiersin.org/article/10.3389/ffunb.2021.742894

Bernardes JP, Stelkens RB, Greig D. 2017. Heterosis in hybrids within and between yeast species. *J Evol Biol* 30:538–548.

Boeva V, Popova T, Bleakley K, Chiche P, Cappo J, Schleiermacher G, Janoueix-Lerosey I, Delattre O, Barillot E. 2012. Control-FREEC: a tool for assessing copy number and allelic content using next-generation sequencing data. *Bioinformatics* 28:423–425.

Boeva V, Zinovyev A, Bleakley K, Vert J-P, Janoueix-Lerosey I, Delattre O, Barillot E. 2011. Control-free calling of copy number alterations in deep-sequencing data using GC-content normalization. *Bioinformatics* 27:268–269.

Bolger AM, Lohse M, Usadel B. 2014. Trimmomatic: a flexible trimmer for Illumina sequence data. *Bioinformatics* 30:2114–2120.

Bolnick DI, Hund AK, Nosil P, Peng F, Ravinet M, Stankowski S, Subramanian S, Wolf JBW, Yukilevich R. 2023. A multivariate view of the speciation continuum. *Evolution* 77:318–328.

Bozdag GO, Ono J, Denton JA, Karakoc E, Hunter N, Leu J-Y, Greig D. 2021. Breaking a species barrier by

788 enabling hybrid recombination. *Current Biology* 31:R180–R181.
789 Brice C, Zhang Z, Bendixsen D, Stelkens R. 2021. Hybridization Outcomes Have Strong Genomic and
790 Environmental Contingencies. *The American Naturalist* 198:E53–E67.
791 Cervantes S, Kesälahti R, Kumpula TA, Mattila TM, Helanterä H, Pyhäjärvi T. 2023. Strong Purifying
792 Selection in Haploid Tissue–Specific Genes of Scots Pine Supports the Masking Theory.
793 *Molecular Biology and Evolution* 40:msad183.
794 Chang S-L, Lai H-Y, Tung S-Y, Leu J-Y. 2013. Dynamic Large-Scale Chromosomal Rearrangements Fuel
795 Rapid Adaptation in Yeast Populations. *PLOS Genetics* 9:e1003232.
796 Chen X, Schulz-Trieglaff O, Shaw R, Barnes B, Schlesinger F, Källberg M, Cox AJ, Kruglyak S, Saunders CT.
797 2016. Manta: rapid detection of structural variants and indels for germline and cancer
798 sequencing applications. *Bioinformatics* 32:1220–1222.
799 Cingolani P, Platts A, Wang LL, Coon M, Nguyen T, Wang L, Land SJ, Lu X, Ruden DM. 2012. A program for
800 annotating and predicting the effects of single nucleotide polymorphisms, SnpEff: SNPs in the
801 genome of Drosophila melanogaster strain w1118; iso-2; iso-3. *Fly (Austin)* 6:80–92.
802 Dagilis AJ, Kirkpatrick M, Bolnick DI. 2019. The evolution of hybrid fitness during speciation. *PLOS*
803 *Genetics* 15:e1008125.
804 Danecek P, Auton A, Abecasis G, Albers CA, Banks E, DePristo MA, Handsaker RE, Lunter G, Marth GT,
805 Sherry ST, et al. 2011. The variant call format and VCFtools. *Bioinformatics* 27:2156–2158.
806 Danecek P, Bonfield JK, Liddle J, Marshall J, Ohan V, Pollard MO, Whitwham A, Keane T, McCarthy SA,
807 Davies RM, et al. 2021. Twelve years of SAMtools and BCFtools. *GigaScience* 10:giab008.
808 Deschênes A, Belleau P, Tuveson DA, Krasnitz A. 2022. Quantifying similarity between copy number
809 profiles with CNVMetrics package. *F1000Research* [Internet] 11. Available from:
810 https://f1000research.com/posters/11-816
811 Dettman JR, Anderson JB, Kohn LM. 2008. Divergent adaptation promotes reproductive isolation among
812 experimental populations of the filamentous fungus Neurospora. *BMC Evol Biol* 8:35.
813 Dettman JR, Sirjusingh C, Kohn LM, Anderson JB. 2007. Incipient speciation by divergent adaptation and
814 antagonistic epistasis in yeast. *Nature* 447:585–588.
815 deVicente MC, Tanksley SD. 1993. Qtl Analysis of Transgressive Segregation in an Interspecific Tomato
816 Cross. *Genetics* 134:585–596.
817 Dieckmann U, Doebeli M, Metz JAJ, Tautz D eds. 2004. Adaptive Speciation. Cambridge: Cambridge
818 University Press Available from: https://www.cambridge.org/core/books/adaptive-
819 speciation/A2413E0B1E5DDAB5C5848F0666468A35
820 Dodd DMB. 1989. Reproductive Isolation as a Consequence of Adaptive Divergence in Drosophila
821 pseudoobscura. *Evolution* 43:1308–1311.
822 Eberlein C, Hénault M, Fijarczyk A, Charron G, Bouvier M, Kohn LM, Anderson JB, Landry CR. 2019.
823 Hybridization is a recurrent evolutionary stimulus in wild yeast speciation. *Nat Commun* 10:923.
824 Filchak KE, Roethele JB, Feder JL. 2000. Natural selection and sympatric divergence in the apple maggot
825 Rhagoletis pomonella. *Nature* 407:739–742.
826 Forejt J, Jansa P. 2023. Meiotic Recognition of Evolutionarily Diverged Homologs: Chromosomal Hybrid
827 Sterility Revisited. *Molecular Biology and Evolution* 40:msad083.
828 Funk DJ, Nosil P, Etges WJ. 2006. Ecological divergence exhibits consistently positive associations with
829 reproductive isolation across disparate taxa. *Proceedings of the National Academy of Sciences*
830 103:3209–3213.
831 Gallone B, Steensels J, Mertens S, Dzialo MC, Gordon JL, Wauters R, Theßeling FA, Bellinazzo F, Saels V,
832 Herrera-Malaver B, et al. 2019. Interspecific hybridization facilitates niche adaptation in beer
833 yeast. *Nat Ecol Evol* 3:1562–1575.
834 Garrison E, Marth G. 2012. Haplotype-based variant detection from short-read sequencing. *arXiv* 1207.
835 Gautier M, Vitalis R, Flori L, Estoup A. 2022. f-Statistics estimation and admixture graph construction

with Pool-Seq or allele count data using the R package poolfstat. *Mol Ecol Resour* 22:1394–1416.
Gerstein AC, Cleathero LA, Mandegar MA, Otto SP. 2011. Haploids adapt faster than diploids across a range of environments. *Journal of Evolutionary Biology* 24:531–540.
Gilchrist C, Stelkens R. 2019. Aneuploidy in yeast: Segregation error or adaptation mechanism? *Yeast* 36:525–539.
Good BH, McDonald MJ, Barrick JE, Lenski RE, Desai MM. 2017. The dynamics of molecular evolution over 60,000 generations. *Nature* 551:45–50.
Gorter FA, Derks MF, van den Heuvel J, Aarts MG, Zwaan BJ, de Ridder D, de Visser JAG. 2017. Genomics of adaptation depends on the rate of environmental change in experimental yeast populations. *Molecular Biology and Evolution* 34:2613–2626.
Gorter FA, Scanlan PD, Buckling A. 2016. Adaptation to abiotic conditions drives local adaptation in bacteria and viruses coevolving in heterogeneous environments. *Biol. Lett.* 12:20150879.
Grant RB, Grant PR. 2003. What Darwin's Finches Can Teach Us about the Evolutionary Origin and Regulation of Biodiversity. *BioScience* 53:965–975.
Greig D, Louis EJ, Borts RH, Travisano M. 2002. Hybrid Speciation in Experimental Populations of Yeast. *Science* 298:1773–1775.
Härer A, Bolnick DI, Rennison DJ. 2021. The genomic signature of ecological divergence along the benthic-limnetic axis in allopatric and sympatric threespine stickleback. *Molecular Ecology* 30:451–463.
Hatfield T, Schluter D. 1999. ECOLOGICAL SPECIATION IN STICKLEBACKS: ENVIRONMENT-DEPENDENT HYBRID FITNESS. *Evolution* 53:866–873.
Hendry AP, Nosil P, Rieseberg LH. 2007. The speed of ecological speciation. *Functional Ecology* 21:455–464.
Hivert V, Leblois R, Petit EJ, Gautier M, Vitalis R. 2018. Measuring Genetic Differentiation from Pool-seq Data. *Genetics* 210:315–330.
Hunter N, Chambers SR, Louis EJ, Borts RH. 1996. The mismatch repair system contributes to meiotic sterility in an interspecific yeast hybrid. *EMBO J* 15:1726–1733.
Irestedt M, Müller I, Thörn F, Joseph L, Nylander J, Guinet B, Valk TV der, Jønsson K. Reticulate and hybrid speciation is promoted by environmental instability in an Indo-Pacific species complex of whistlers (Aves: Pachycephala). Available from: https://www.authorea.com/doi/full/10.22541/au.173053090.08198521?commit=f442f52dffaefd5b78602e94558c1591a8dff4e5; accepted for publication in Molecular Ecology, Special Issue on Genomics of Speciation.
Jarrett BJM, Downing PA, Svensson EI. 2024. Divergent selection and plasticity shape reproductive isolation at the onset of speciation. :2024.09.23.614431. Available from: https://www.biorxiv.org/content/10.1101/2024.09.23.614431v1
Johnson MS, Desai MM. 2022. Mutational robustness changes during long-term adaptation in laboratory budding yeast populations.Cooper VS, Walczak AM, Miller C, editors. *eLife* 11:e76491.
Kirkpatrick M, Ravigné V. 2002. Speciation by natural and sexual selection: models and experiments. *Am Nat* 159 Suppl 3:S22-35.
Kosheleva K, Desai MM. 2018. Recombination Alters the Dynamics of Adaptation on Standing Variation in Laboratory Yeast Populations. *Mol Biol Evol* 35:180–201.
Lenski RE, Rose MR, Simpson SC, Tadler SC. 1991. Long-Term Experimental Evolution in Escherichia coli. I. Adaptation and Divergence During 2,000 Generations. *The American Naturalist* 138:1315–1341.
Leu J-Y, Chang S-L, Chao J-C, Woods LC, McDonald MJ. 2020. Sex alters molecular evolution in diploid experimental populations of S. cerevisiae. *Nat Ecol Evol* 4:453–460.
Li H, Durbin R. 2009. Fast and accurate short read alignment with Burrows–Wheeler transform.

Bioinformatics 25:1754–1760.
Li J, Vázquez-García I, Persson K, González A, Yue J-X, Barré B, Hall MN, Long A, Warringer J, Mustonen V, et al. 2019. Shared Molecular Targets Confer Resistance over Short and Long Evolutionary Timescales. *Molecular Biology and Evolution* 36:691–708.
Liu Y, Ma G, Gao Z, Li J, Wang J, Zhu X, Ma R, Yang J, Zhou Y, Hu K, et al. 2022. Global chromosome rearrangement induced by CRISPR-Cas9 reshapes the genome and transcriptome of human cells. *Nucleic Acids Research* 50:3456–3474.
Louder MIM, Justen H, Kimmitt AA, Lawley KS, Turner LM, Dickman JD, Delmore KE. 2024. Gene regulation and speciation in a migratory divide between songbirds. *Nat Commun* 15:98.
Mayr E. 1947. Ecological Factors in Speciation. *Evolution* 1:263–288.
McDonald MJ, Rice DP, Desai MM. 2016. Sex speeds adaptation by altering the dynamics of molecular evolution. *Nature* 531:233–236.
McKinnon JS, Mori S, Blackman BK, David L, Kingsley DM, Jamieson L, Chou J, Schluter D. 2004. Evidence for ecology's role in speciation. *Nature* 429:294–298.
Meyer JR, Dobias DT, Medina SJ, Servilio L, Gupta A, Lenski RE. 2016. Ecological speciation of bacteriophage lambda in allopatry and sympatry. *Science* 354:1301–1304.
Michel AP, Sim S, Powell THQ, Taylor MS, Nosil P, Feder JL. 2010. Widespread genomic divergence during sympatric speciation. *Proceedings of the National Academy of Sciences* 107:9724–9729.
Muenzner J, Trébulle P, Agostini F, Zauber H, Messner CB, Steger M, Kilian C, Lau K, Barthel N, Lehmann A, et al. 2024. Natural proteome diversity links aneuploidy tolerance to protein turnover. *Nature* 630:149–157.
Mukherjee V, Lind U, St. Onge RP, Blomberg A, Nygård Y. 2021. A CRISPR Interference Screen of Essential Genes Reveals that Proteasome Regulation Dictates Acetic Acid Tolerance in Saccharomyces cerevisiae. *mSystems* 6:10.1128/msystems.00418-21.
Müller I, Thörn F, Rajan S, Olsen R-A, Ericson P, Peona V, Smith B, Maiah G, Koane B, Iova B, et al. Ephemeral speciation in a New Guinean honeyeater complex (Aves: Melidectes). Available from: https://www.authorea.com/doi/full/10.22541/au.173639442.28305532?commit=c6fffa9cc0ca71d3e44f2de72f5001a07ea2ab20; accepted for publication in Molecular Ecology, Special Issue on Genomics of Speciation.
Munar-Delgado G, Pulido F, Edelaar P. 2024. Performance-based habitat choice can drive rapid adaptive divergence and reproductive isolation. *Current Biology* 34:5564-5569.e4.
Nosil P. 2012. Ecological Speciation. Oxford University Press Available from: https://academic.oup.com/book/5499
Nosil P, Crespi BJ. 2006. Experimental evidence that predation promotes divergence in adaptive radiation. *Proceedings of the National Academy of Sciences* 103:9090–9095.
Nosil P, Feder JL. 2012. Genomic divergence during speciation: causes and consequences. *Philosophical Transactions of the Royal Society B: Biological Sciences* 367:332–342.
Nosil P, Schluter D. 2011. The genes underlying the process of speciation. *Trends Ecol Evol* 26:160–167.
Okonechnikov K, Conesa A, García-Alcalde F. 2016. Qualimap 2: advanced multi-sample quality control for high-throughput sequencing data. *Bioinformatics* 32:292–294.
Ono J, Gerstein AC, Otto SP. 2017. Widespread Genetic Incompatibilities between First-Step Mutations during Parallel Adaptation of Saccharomyces cerevisiae to a Common Environment. *PLOS Biology* 15:e1002591.
Persson K, Onyema VO, Nwafor IP, Peri KVR, Otti C, Nnaemeka P, Onyishi C, Okoye S, Moneke A, Amadi O, et al. 2024. Lactose-assimilating yeasts with high fatty acid accumulation uncovered by untargeted bioprospecting. *Applied and Environmental Microbiology* 0:e01615-24.
Persson K, Stenberg S, Tamás MJ, Warringer J. 2022. Adaptation of the yeast gene knockout collection is near-perfectly predicted by fitness and diminishing return epistasis. *G3*

Genes|Genomes|Genetics 12:jkac240.
Peter J, De Chiara M, Friedrich A, Yue J-X, Pflieger D, Bergström A, Sigwalt A, Barre B, Freel K, Llored A, et al. 2018. Genome evolution across 1,011 Saccharomyces cerevisiae isolates. *Nature* 556:339–344.
R Core Team. 2023. R: A Language and Environment for Statistical Computing. Available from: https://www.R-project.org/
Rainey PB, Travisano M. 1998. Adaptive radiation in a heterogeneous environment. *Nature* 394:69–72.
Rogers DW, McConnell E, Ono J, Greig D. 2018. Spore-autonomous fluorescent protein expression identifies meiotic chromosome mis-segregation as the principal cause of hybrid sterility in yeast. *PLOS Biology* 16:e2005066.
Rundle HD, Nagel L, Wenrick Boughman J, Schluter D. 2000. Natural selection and parallel speciation in sympatric sticklebacks. *Science* 287:306–308.
Sawada A, Iwasaki T, Akatani K, Takagi M. 2022. Mate choice for body size leads to size assortative mating in the Ryukyu Scops Owl Otus elegans. *Ecology and Evolution* 12:e9578.
Schluter D. 2001. Ecology and the origin of species. *Trends Ecol Evol* 16:372–380.
Schluter D. 2009. Evidence for Ecological Speciation and Its Alternative. *Science* 323:737–741.
Scopel EFC, Hose J, Bensasson D, Gasch AP. 2021. Genetic variation in aneuploidy prevalence and tolerance across Saccharomyces cerevisiae lineages. *Genetics* 217:iyab015.
Shapira R, Levy T, Shaked S, Fridman E, David L. 2014. Extensive heterosis in growth of yeast hybrids is explained by a combination of genetic models. *Heredity (Edinb)* 113:316–326.
Sparks MM, Kraft JC, Blackstone KMS, McNickle GG, Christie MR. 2022. Large genetic divergence underpins cryptic local adaptation across ecological and evolutionary gradients. *Proceedings of the Royal Society B: Biological Sciences* 289:20221472.
Stankowski S, Ravinet M. 2021. Defining the speciation continuum. *Evolution* 75:1256–1273.
Stelkens R. 2024. A microbial perspective on speciation. *Evolutionary Journal of the Linnean Society* 3:kzae023.
Stelkens RB, Brockhurst MA, Hurst GDD, Miller EL, Greig D. 2014. The effect of hybrid transgression on environmental tolerance in experimental yeast crosses. *J. Evol. Biol.* 27:2507–2519.
Stenberg S, Li J, Gjuvsland AB, Persson K, Demitz-Helin E, González Peña C, Yue J-X, Gilchrist C, Ärengård T, Ghiaci P, et al. 2022. Genetically controlled mtDNA deletions prevent ROS damage by arresting oxidative phosphorylation.Gruber J, Tyler JK, Toledano MB, editors. *eLife* 11:e76095.
Struck TH, Feder JL, Bendiksby M, Birkeland S, Cerca J, Gusarov VI, Kistenich S, Larsson K-H, Liow LH, Nowak MD, et al. 2018. Finding Evolutionary Processes Hidden in Cryptic Species. *Trends in Ecology & Evolution* 33:153–163.
Tange O. 2011. Gnu parallel-the command-line power tool. *Usenix Mag* 36:42.
Thompson KA, Brandvain Y, Coughlan JM, Delmore KE, Justen H, Linnen CR, Ortiz-Barrientos D, Rushworth CA, Schneemann H, Schumer M, et al. 2023. The Ecology of Hybrid Incompatibilities. *Cold Spring Harb Perspect Biol*:a041440.
Tusso S, Nieuwenhuis BPS, Weissensteiner B, Immler S, Wolf JBW. 2021. Experimental evolution of adaptive divergence under varying degrees of gene flow. *Nat Ecol Evol* 5:338–349.
Villa SM, Altuna JC, Ruff JS, Beach AB, Mulvey LI, Poole EJ, Campbell HE, Johnson KP, Shapiro MD, Bush SE, et al. 2019. Rapid experimental evolution of reproductive isolation from a single natural population. *Proceedings of the National Academy of Sciences* 116:13440–13445.
Westram AM, Stankowski S, Surendranadh P, Barton N. 2022. What is reproductive isolation? *Journal of Evolutionary Biology* 35:1143–1164.
Zackrisson M, Hallin J, Ottosson L-G, Dahl P, Fernandez-Parada E, Ländström E, Fernandez-Ricaud L, Kaferle P, Skyman A, Stenberg S, et al. 2016. Scan-o-matic: High-Resolution Microbial Phenomics at a Massive Scale. *G3 Genes|Genomes|Genetics* 6:3003–3014.

980 Zhang Z, Bendixsen DP, Janzen T, Nolte AW, Greig D, Stelkens R. 2020. Recombining Your Way Out of
981 Trouble: The Genetic Architecture of Hybrid Fitness under Environmental Stress. *Molecular*
982 *Biology and Evolution* 37:167–182.
983

984 **Data Accessibility and Benefit-Sharing Section**

985 Phenotypic data are available in Table S1. The raw sequences were deposited in the European
986 Nucleotide Archive, parental populations are available at accession number PRJEB46680, while hybrids
987 are available at accession number PRJEB83568. The code used for analyses and plotting are available at
988 https://github.com/devinbendixsen/EvolvingRI. Benefits from this research accrue from the sharing of
989 our data and results on public databases as described above.

990

991 **Author Contributions**

992 Conceived research: Rike Stelkens; Designed research: Rike Stelkens, Ciaran Gilchrist; Performed
993 research: Devin P. Bendixsen, Ciaran Gilchrist, Chloé Haberkorn, Karl Persson; Contributed new reagents
994 or analytical tools: Karl Persson, Jonas Warringer; Data analysis: Devin P. Bendixsen, Chloé Haberkorn,
995 Karl Persson; Writing: Rike Stelkens, Devin P. Bendixsen, Chloé Haberkorn, Ciaran Gilchrist; Funding
996 acquisition: Rike Stelkens, Devin P. Bendixsen, Cecilia Geijer, Jonas Warringer.